

CHARLES UNIVERSITY

FACULTY OF PHARMACY IN HRADEC KRÁLOVÉ

DPT. OF PHARMACEUTICAL CHEMISTRY AND PHARMACEUTICAL ANALYSIS



Synthesis and Evaluation of Novel Quinazolones as Potential Antimicrobial Compounds

Diploma Thesis

Head of Department: Prof. PharmDr. Martin Doležal, Ph.D.

Supervisor: Assoc. Prof. PharmDr. Jan Zitko, Ph.D.

Consultant: Ghada Bouz, Ph.D.

Candidate: Hanieh Kamangar

Hradec Králové, 2024

Acknowledgement

I would like to thank my consultant Ghada Bouz, Ph.D., my supervisor doc. PharmDr. Jan Zitko, Ph.D., and our head of department, prof. PharmDr. Martin Doležal, Ph.D. for their guidance and support, and finally my family for their endless love and trust in my abilities.

The study was supported by “The project National Institute of virology and bacteriology (Programme EXCELES, ID Project No. LX22NPO5103) - Funded by the European Union - Next Generation EU.”

Supported by grant SVV 260 666

„I declare that this thesis is my original author's work, which has been composed solely by myself (under the guidance of my consultant). All the literature and other resources from which I drew information are cited in the list of used literature and are quoted in the paper. The work has not been used to get another or the same title. “

Hanieh Kamangar

Hradec Králové, 2024

TABLE OF CONTENTS

1.	list of abbreviations	6
2.	aim of work.....	7
3.	introduction and design rationale	8
3.1.	Staphylococcus aureus (SA)	8
3.2.	Methicillin-resistant Staphylococcus aureus (MRSA).....	8
3.3.	Clinically available antistaphylococcal agents.....	9
3.4.	Quinazolines	13
3.5.	Quinazolinone-containing drugs in clinical use.....	17
3.6.	Design rationale of thesis work	19
4.	EXPERIMENTAL PART	25
4.1.	Instrumentation.....	25
4.2.	Chemistry	26
4.2.1.	General procedure	26
4.2.2.	Final compounds	28
	Code: GDM18.....	29
	Code: GDM29.....	30
	Code: GDM32	31
	Code: GDM31	32
	Code: GDM20.....	33
	Code: GDM22.....	34
	Code: GDM30.....	35
	Code: GDM27	36
	Code: GDM24.....	37
	Code: GDM35.....	38
	Code: GDM26.....	39
4.3.	Biological Assays	40
4.3.1.	<i>In Vitro</i> Antibacterial Activity Evaluation	40
4.3.2.	<i>In Vitro</i> Activity Evaluation Against <i>Mycobacterium tuberculosis</i> , <i>Mycobacterium kansasii</i> , and <i>Mycobacterium avium</i>	41

4.3.3.	<i>In Vitro</i> Activity Evaluation Against <i>Mycobacterium smegmatis</i> and <i>Mycobacterium aurum</i>	42
4.3.4.	<i>In Vitro</i> Antifungal Activity Evaluation	43
4.4.	Results and discussion	44
4.4.1.	Chemistry	44
4.4.2.	Predicted pharmacokinetics, drug-likeness, and medicinal chemistry features 45	
4.4.3.	Antibacterial activity	50
4.4.4.	Antimycobacterial Activity	51
4.4.5.	Antifungal activity	54
4.4.6.	Comparison to structurally related compounds reported in the diploma work of my colleague Asal Askari	55
5.	CONCLUSIONS	57
6.	ABSTRAKT (CZECH)	58
7.	ABSTRACT (ENGLISH)	59
8.	REFERENCES	60

1. LIST OF ABBREVIATIONS

AQs	Antistaphylococcal quinazolones
<i>E. coli</i>	<i>Escherichia coli</i>
<i>EF</i>	<i>Enterococcus faecalis</i>
HVISA	heterogeneous vancomycin-intermediate <i>Staphylococcus aureus</i>
MOA	Mechanism of Action
MRSA	methicillin-resistant <i>Staphylococcus aureus</i>
MSSA	methicillin-susceptible <i>Staphylococcus aureus</i>
PBP	penicillin binding protein
<i>SA</i>	<i>Staphylococcus aureus</i>
<i>SE</i>	<i>Staphylococcus epidermidis</i>
<i>TB</i>	Tuberculosis
WHO	World Health Organization
VISA	vancomycin-intermediate <i>Staphylococcus aureus</i>
VRE	vancomycin-resistant <i>Enterococci</i>
VRSA	vancomycin-resistant <i>Staphylococcus aureus</i>

2. AIM OF WORK

Staphylococcus aureus (SA) is a major cause of infections that can be fatal.[1] Compared to patients infected with non-resistant bacteria, those with methicillin-resistant SA (MSRA) infections have a 64% increased risk of dying.[2] Developing novel agents is one way to control SA infections. It has been documented in the literature that compounds with quinazolinone display a wide range of distinct pharmacological actions.[3] Antistaphylococcal quinazolones (AQs) have previously been shown to have established structure-activity relationships. Using molecular docking, colleagues in our research group integrated long-term understanding of antimicrobials and published research to design new, potentially active antibiotics (AQs) that specifically target penicillin binding protein (PBP) 2a of *S. aureus*. The starting material was prepared by heating 2-amino-4-chlorobenzoic acid with acetic anhydride. The latter product was then reacted with several substituted chlorinated benzylamines (see figure 1) to yield final compounds. Final compounds were evaluated for their antimicrobial activity against SA and -as complementary testing- screened against other bacteria, fungi, and mycobacteria of clinical importance.

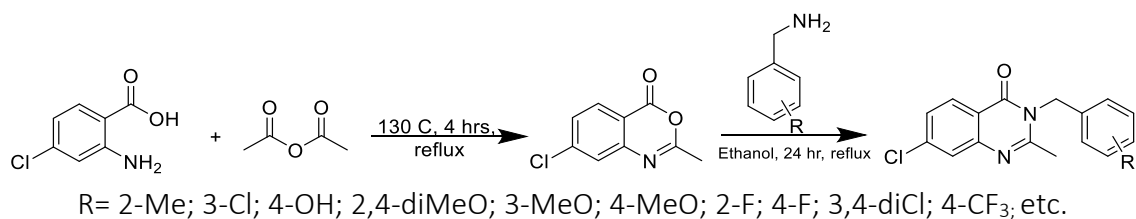


Figure 1. Synthetic scheme of title compounds.

3. INTRODUCTION AND DESIGN RATIONALE

3.1. *Staphylococcus aureus* (SA)

Staphylococcus aureus (SA) is a gram-positive bacterium that is cocci-shaped and can grow both aerobically and anaerobically. It is one of the main pathogens causing life-threatening infections and has the ability to form biofilms. Due to the increased resistance, the treatment is challenging.[4] SA can be found on skin and mucous membranes as normal flora, but it can cause a number of potentially dangerous illnesses if it gets into the bloodstream or internal tissues. They are typically transmitted by direct contact. The most common SA infections are skin infections, often leading to the formation of abscesses. In addition, the bacteria can travel through the bloodstream and infect other organs, such as heart valves (endocarditis), bones (osteomyelitis) and lungs (pneumonia).[1] [5]

SA can generate a range of endotoxins and other toxins that can induce inflammatory reactions and activate inflammatory cells, including keratinocytes, helper T cells, innate lymphoid cells, macrophages, dendritic cells, mast cells, neutrophils, eosinophils, and basophils. Numerous cytokines can be expressed by activated inflammatory cells, which can then trigger an inflammatory response. Moreover, SA can cause host cell death by autophagy, pyroptosis, apoptosis, necroptosis, and other mechanisms.[6]

3.2. Methicillin-resistant *Staphylococcus aureus* (MRSA)

The development of resistance in organisms that are common human pathogens has significantly increased from 1950s.[7] The range of antimicrobials that can be utilized to treat pathogens has decreased due to increasing resistance. Certain classes of organisms also require the development of new antimicrobials. There are extremely few antimicrobials available to treat mycobacterial and fungal infections. Furthermore, microbes are ever-evolving, continually seeking new habitats, developing survival strategies, and adjusting to novel environments. It's critical to keep looking for anti-infective drugs that can be used to treat infections since new infectious diseases are always being discovered and old pathogens are developing new mechanisms of resistance and pathogenesis. Maintaining the fight against infectious diseases will require

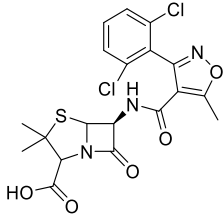
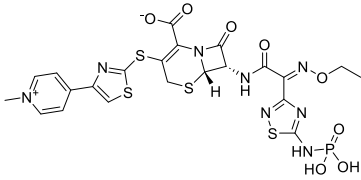
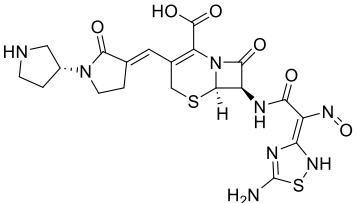
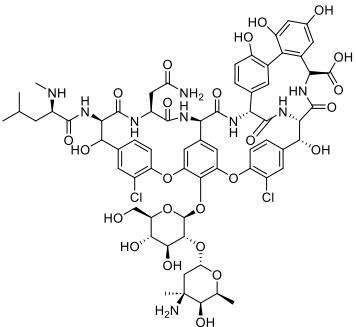
the development of new drug classes, medications with fewer side effects, and medications that require shorter treatment durations.[8] [9]

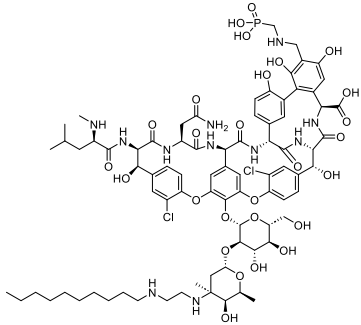
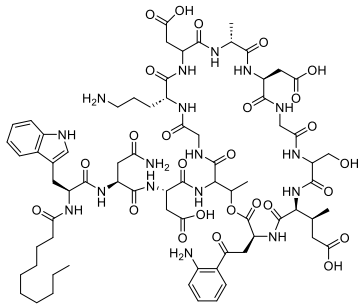
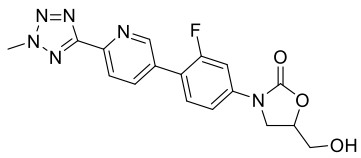
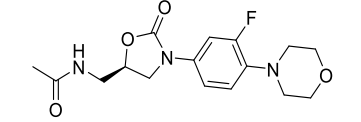
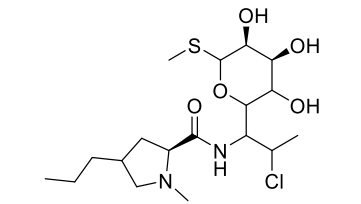
SA can be either methicillin-susceptible (MSSA), methicillin-resistant (MRSA), vancomycin-intermediate (VISA), heterogeneous vancomycin-intermediate (HVISA) and vancomycin-resistant (VRSA). MRSA is the most common cause of antibiotic-resistant health care-associated infections. Due to their major health threats the world health organization (WHO) lists *SA*, MRSA, VISA, and VRSA on the priority pathogens list for research and development of new antibiotics.[10] Penicillin-binding proteins (PBPs), which are enzymes involved in the formation of cell walls, are the target of beta-lactam antibiotics.[11] In addition to the four PBPs that *S. aureus* naturally possesses, MRSA has obtained PBP 2a(PDB id: 6Q9N), which provides broad resistance to beta-lactam antibiotics when faced with their challenge.[12] Clinical treatment for *S. aureus* infections used to mostly consist of β -lactam antibiotics. However, MRSA exhibits resistance against the majority of β -lactam antibiotics. [11–13] Antibiotics like ceftaroline and ceftobiprole, which are more recent cephalosporines, have anti-MRSA properties but they require intravenous infusions every 8–12 hours.[14] Because allostery regulates the closed active-site shape of this enzyme, it can avoid inhibition by β -lactams. [15–16] Even though various antibiotics have been brought to the clinic to treat MRSA,[17] only the oxazolidinones—linezolid and tedizolid—are orally administered.[18]

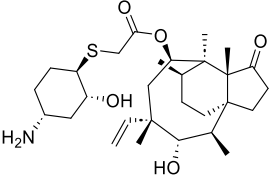
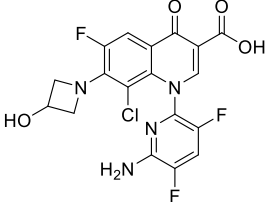
3.3. Clinically available antistaphylococcal agents

Several antimicrobials have been in use for a long time to treat *SA* infections. Table 1 summarizes selected antistaphylococcal agents with their mechanism of action and chemical structures.

Table 1: Clinically available antistaphylococcal agents

Agent	MOA	Structure
<p>Penicillins (e.g. Oxacillin)</p>	<p>Inhibits the third and final stage of bacterial cell wall formation by attaching specific penicillin-binding proteins (PBPs) inside the bacterial cell wall and active against gram-positive and gram-negative aerobic and anaerobic bacteria.[19]</p>	 <p>The image shows the chemical structure of Oxacillin, a penicillinase-resistant penicillin. It features a central beta-lactam ring fused to a five-membered thiazolidine ring. The thiazolidine ring has a tert-butyl group at the 4-position and a carboxylic acid group at the 3-position. The beta-lactam ring is substituted at the 6-position with a 5-chloro-2-methyl-1,2,4-oxazol-5-yl group.</p>
<p>Ceftaroline fosamil (prodrug)</p>	<p>Inhibits bacteria from synthesising their cell walls by attaching to penicillin-binding proteins (PBPs). Because of the mecA gene, which codes for a mutated form of PBP 2a with a low binding affinity for beta-lactam antibiotics, MRSA is resistant to practically all of them. Ceftaroline binds to MRSA PBPs 1-4 and PBP 2a with an equal amount of strength.[19] [20]</p>	 <p>The image shows the chemical structure of Ceftaroline fosamil, a cephalosporin antibiotic. It consists of a cephalosporin core with a fosfomic acid group attached to the 3-position of the dihydrothiazine ring. The core is substituted with a 4-methyl-5-(1-methyl-4-pyridin-2-yl-1H-imidazol-2-ylthio)phenyl group at the 7-position and a 2-ethoxyethyl group at the 4-position of the dihydrothiazine ring.</p>
<p>Ceftobiprole</p>	<p>Binding to penicillin-binding proteins (PBPs) and inhibit their transpeptidase activity, which is essential for the synthesis of the peptidoglycan layer of the bacterial cell wall. They are active against Gram-positive bacteria, including methicillin-resistant <i>Staphylococcus aureus</i> (MRSA), Ceftobiprole binds to PBP2a.[19] [21]</p>	 <p>The image shows the chemical structure of Ceftobiprole, a cephalosporin antibiotic. It features a cephalosporin core with a 2-amino-5-nitro-1,3,4-thiadiazol-5-yl group at the 3-position of the dihydrothiazine ring. The core is substituted with a 4-(2-((2S,5S)-2-oxopyrrolidin-5-yl)ethyl)phenyl group at the 7-position and a carboxylic acid group at the 4-position of the dihydrothiazine ring.</p>
<p>Vancomycin</p>	<p>Inhibits synthesis of cell wall peptidoglycan and inhibits bacterial cell membrane permeability. It is a glycopeptide antibiotic, active against Gram-positive bacteria, including penicillin-resistant <i>pneumococci</i> and MRSA (methicillin-resistant <i>Staphylococcus aureus</i>), among others, particularly since their introduction.[22] [23]</p>	 <p>The image shows the chemical structure of Vancomycin, a glycopeptide antibiotic. It is a complex molecule consisting of a central vanillic acid core linked to a long chain of amino acids, including tyrosine, threonine, and valine, which are further substituted with various functional groups like hydroxyl, methyl, and amino groups.</p>

Telavancin	Inhibits polymerization of <i>N</i> -acetylmuramic acid (NAM) and <i>N</i> -acetylglucosamine (NAG) and cross-linking of peptidoglycan by binding to D-Ala-D-Ala. inhibition of bacterial cell wall synthesis occurs. It has bactericidal activity against Methicillin-resistant <i>Staphylococcus aureus</i> (MRSA) and other gram-positive bacteria.[24] [25]	 <p>The chemical structure of Telavancin is a complex molecule featuring a central chromane core. It has multiple hydroxyl groups, a chlorine atom, and a phosphate group at the top. A long alkyl chain is attached to the bottom of the structure.</p>
Daptomycin	Attaches itself to the membranes of the bacteria, causing the membrane to rapidly depolarize because of potassium efflux and the resulting interruption of DNA, RNA, and protein synthesis; this leads to a concentration-dependent, rapid death of the bacteria. It is active against Gram-positive bacteria, including methicillin-susceptible and -resistant <i>Staphylococcus aureus</i> (MSSA/MRSA) and vancomycin-resistant <i>Enterococci</i> (VRE).[26] [27]	 <p>The chemical structure of Daptomycin is a cyclic lipopeptide. It consists of a 14-membered macrocyclic ring with several side chains, including a long alkyl chain, a cyclohexane ring, and a phenyl ring. There are also several hydroxyl and amide groups.</p>
Tedizolid	Inhibits protein synthesis by binding to the 50S ribosomal subunit and active against Gram-positive bacteria, including methicillin-resistant <i>Staphylococcus aureus</i> (MRSA).[28] [29]	 <p>The chemical structure of Tedizolid features a central pyridine ring substituted with a diazole group, a fluorine atom, and a morpholine ring. A hydroxymethyl group is attached to the morpholine ring.</p>
Linezolid	Inhibits protein synthesis by interacting with the 50S subunit. It is a bacteriostatic against both <i>Staphylococci</i> and <i>Enterococci</i> and bactericidal against most isolates of <i>Streptococci</i> .[28] [23]	 <p>The chemical structure of Linezolid consists of a morpholine ring substituted with a fluorine atom and a piperazine ring. A hydroxyl group is attached to the morpholine ring, and a carbonyl group is attached to the piperazine ring.</p>
Clindamycin	Inhibits protein synthesis by interacting with the 50S subunit. It is active against several gram-positive aerobic bacteria, as well as gram-positive and gram-negative anaerobes.[30] [31]	 <p>The chemical structure of Clindamycin is a complex molecule with a central pyridine ring. It has a hydroxyl group, a chlorine atom, and a long alkyl chain. There are also several hydroxyl and amide groups.</p>

Lefamulin	<p>Inhibits protein synthesis by interacting with the 50S subunit. It is active against gram-positive and atypical microbes (for example, <i>Streptococcus pneumoniae</i>, <i>Legionella pneumophila</i>, <i>Mycoplasma pneumoniae</i>, <i>Haemophilus influenzae</i>, and <i>Chlamydomydia pneumoniae</i>). Lefamulin also shows activity against SA, methicillin-resistant <i>Staphylococcus aureus</i>, and vancomycin-resistant <i>Enterococcus faecium</i>. [32] [33]</p>	 <p>The chemical structure of Lefamulin is a complex polycyclic molecule. It features a central bicyclic core with a sulfur atom in a five-membered ring. Attached to this core are a cyclohexane ring with an amino group (H₂N), a hydroxyl group (OH), and a thioether linkage to a propyl chain. The propyl chain is further substituted with a methyl group and a carbonyl group (C=O) that is part of a larger ring system. The molecule also contains several other rings, including a five-membered ring with a carbonyl group and a six-membered ring with a hydroxyl group (HO).</p>
Delafloxacin	<p>Inhibits bacterial DNA gyrase and topoisomerase IV. It is active against Gram-positive organisms <i>Staphylococcus aureus</i> (including methicillin-resistant and methicillin-susceptible isolates), <i>Staphylococcus haemolyticus</i>, <i>Staphylococcus lugdunensis</i>, <i>Streptococcus agalactiae</i>, <i>Streptococcus anginosus</i> Group (including <i>Streptococcus anginosus</i>, <i>Streptococcus intermedius</i>, and <i>Streptococcus constellatus</i>), <i>Streptococcus pyogenes</i>, and <i>Enterococcus faecalis</i> also the Gram-negative organisms <i>Escherichia coli</i>, <i>Enterobacter cloacae</i>, <i>Klebsiella pneumoniae</i>, and <i>Pseudomonas aeruginosa</i>. [34]</p>	 <p>The chemical structure of Delafloxacin is a complex heterocyclic molecule. It features a central pyridine ring system with a carboxylic acid group (COOH) and a chlorine atom (Cl). Attached to this system are a fluorine atom (F), a hydroxyl group (OH), and a nitrogen atom that is part of a five-membered ring. The molecule also contains a six-membered ring with a fluorine atom (F) and a nitrogen atom with an amino group (H₂N).</p>

3.4. Quinazolines

Heterocyclic compounds have a great importance in medicinal chemistry. One of the most important heterocycles in medicinal chemistry are quinazolines, possessing wide spectrum of biological activities like antibacterial, antifungal, anticonvulsant, anti-inflammatory, anti-HIV, anticancer and analgesic. This skeleton is an important pharmacophore considered as a privileged structure.[35–36] Thanks to the stability of its nucleus, 4-(3*H*)quinazolinone and its derivatives help in the development of more new drugs with good bioavailability and outstanding *in vitro* and *in vivo* potency against various kinds of infections.[3]

Within the class of fused heterocycles found in over 200 naturally occurring alkaloids, the 4-(3*H*)quinazolinone and its derivatives are of great significance. The previous name for this fused bicyclic compound was benzo-1,3-diazine. Weddige first suggested the name quinazoline (German: Chinazolin) for this molecule after seeing that it was isomeric with quinoxaline and cinnoline.[37] Table 2 provides a brief history of the quinazoline moiety's evolution. Even though quinazoline could be synthesized in good yield by oxidizing 3,4-dihydroquinazoline with alkaline potassium ferricyanide as early as 1903,[38] it wasn't until 1950 that medicinal chemists began to show interest in the moiety due to the elucidation of 3-[β -keto-g-(3-hydroxy-2-piperidyl)-propyl]-4-quinazolone, an alkaloid quinazolinone. *Dichroa febrifuga*, a traditional Chinese herb, yielded this quinazolinone derivative, which was proven to be beneficial against malaria.[39] More than 300000 quinazoline structural compounds are found in SciFinder, remarkably it was discovered that about 40000 compounds possessed biological activity.[40]

Table 2: Timeline representing the development of quinazoline scaffold. The table was taken without modifications from [40]

Year	Discovery
1869	Griess prepared the first quinazoline derivative, 2cyano-3,4-dihydro-4-oxoquinazoline
1887	The name quinazoline (German:Chinazolin)was first proposed for this compound by Weddige
1889	Paal and Bush suggested the numbering of quinazoline ring system
1903	More satisfactory synthesis of quinazoline was subsequently devised
1951	The first renowned quinazoline marketed drug-Methaqualone is used for its sedative-hypnotic effects
1957	Chemistry of quinazoline was reviewed by Williamson
1959	Chemistry of quinazoline was further reviewed by Lindquist
1963	Brought up to date by Armarego in 1963
1960-2010	More than hundred drugs containing Quinazoline moieties have made their way to the market

The most significant class of compounds with a quinazoline nucleus is made up of molecules with hydroxyl groups (or tautomeric oxo groups) next to heterocyclic nitrogen atoms in positions 2 or 4 of the quinazoline ring (Figure 2). Compounds with a functional group that may be readily generated from and converted to a hydroxyl group, such as amino, thioethers, selenium, alkoxy, and aryloxy, are also taken into consideration in this class. Two types of compounds can be identified based on the location of the keto or oxo group: 2-(1*H*) quinazolinones and 4-(3*H*)quinazolinones.[41] Therefore, 4-hydroxyquinazoline, also known as 4-(3*H*)quinazolone or just 4-quinazolinone, is a

frequent term for this compound. Based on the substituents positioned at various positions, the main quinazolinone subclasses are shown in Figure 2. The most common of the four quinazolinone molecules is 4-(3*H*)quinazolinone, which can be found in several potential biosynthetic routes either as primary products or as intermediates. This is partially because the 2-(1*H*)quinazolinone is mostly a byproduct of anthranilonitrile, or benzamide with nitriles, whereas the structure is generated from the anthranilates. Quinazoline precursors can be transformed into 4-(3*H*)quinazolinone by the process of auto-oxidation.[40]

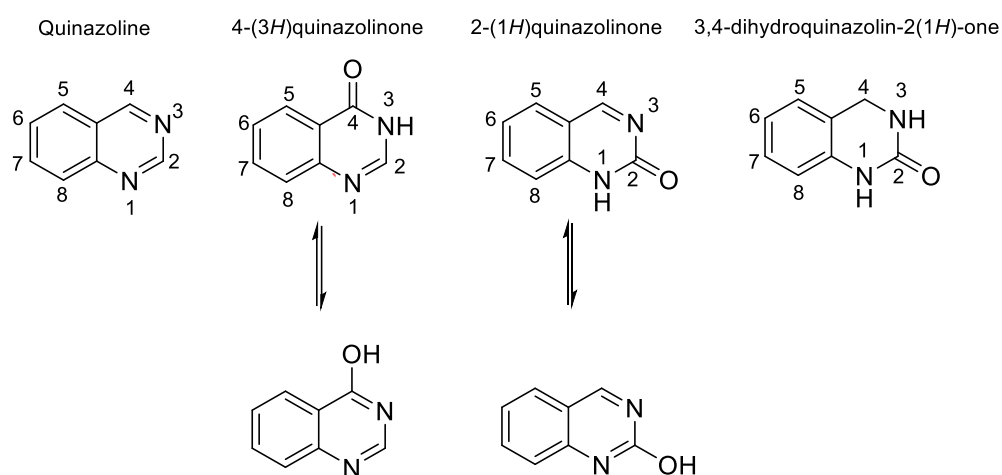


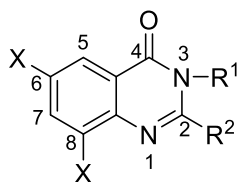
Figure 2. General structure of quinazoline and its subclasses.

Prior research has discovered and validated the stability of the quinazolinone ring against oxidation, reduction, and hydrolysis reactions. There have been no reports of procedures involving ring destruction by straightforward chemical oxidation up to this point. Medicinal chemists have been motivated to synthesize novel potential drugs by adding several bioactive moieties to the quinazolinone nucleus due to its stability. [40]

Among their wide pharmacological application, in this work we will focus on their antimicrobial activity. By interacting with DNA structures and cell walls, quinazolinone derivatives have antibacterial properties, particularly against gram positive bacteria and fungi.

Studies of quinazolinone derivatives' structure-activity relationships have been reported in several publications. These studies have shown that quinazolinone derivatives' antimicrobial activities can be enhanced by substitution at positions 2 and 3, the presence

of halogen atoms at position 6 and 8, and reacting primary amine or substituted amine with oxo group at the quinazolinone ring's position 4 to form Schiff bases (Fig. 3). It is necessary for antibacterial activity to have a substituted aromatic ring at position 3 and methyl, amino, or thiol groups at position 2.[42–46]



R¹ = substituted aromatic ring

R² = methyl, amino, thiol

X = halogen

Figure 3. Quinazolinone basic structure with favorable substituents for antimicrobial activity.

According to SAR studies, compounds that were substituted at position 6 of the quinazolinone ring demonstrated significant antibacterial activity when compared to compounds that were substituted at positions 5 or 8. While the activity was unaffected by electron-donating or electron-withdrawing groups at position 6, the nitro group was generally tolerated and increased the antibacterial activity's potency. In certain compounds, the antibacterial activity has been maintained when the 6-methyl group was substituted with the 6-nitro group. The antibacterial activity persisted even when the 2-oxopropylthio moiety was swapped out for the 2-phenylcarbonylmethylthio moiety. The 3-benzyl-2-((3-nitropyridin-2-yl)thio)quinazolin-4(3*H*)-one and 3-benzyl-2-((2-oxo-2-phenylethyl)thio)quinazolin-4(3*H*)-one derivatives have been found from the pharmacological tests to be desirable antibacterial candidates for potential future medication development.[47] [48]

To sum up, the SAR studies indicated that, as shown in Fig. 4, the benzyl or pyridine-3-ylmethyl groups were important for antibacterial action.

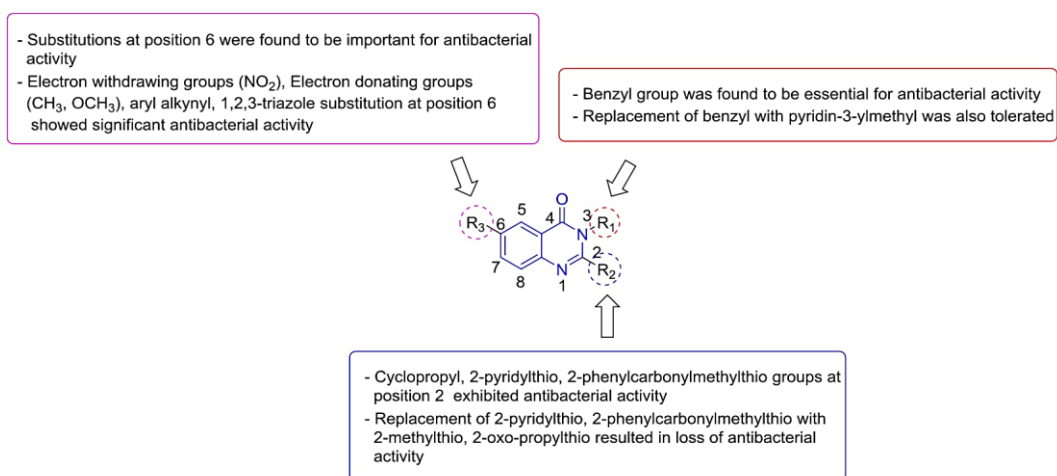


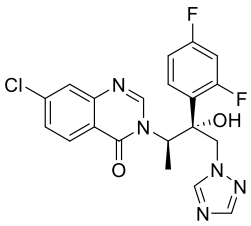
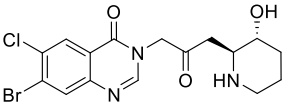
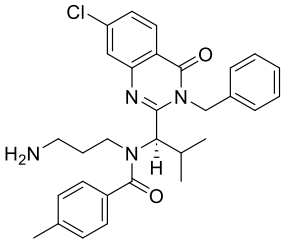
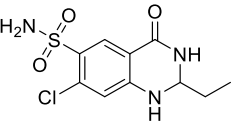
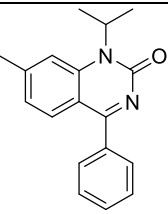
Figure 4: Brief SAR of antistaphylococcal 3-*N*-substituted 4(3*H*)-quinazolinone derivatives. Taken from [3]

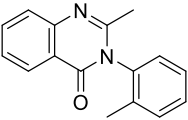
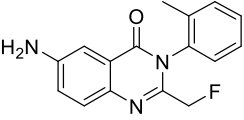
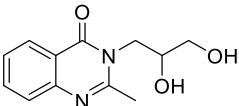
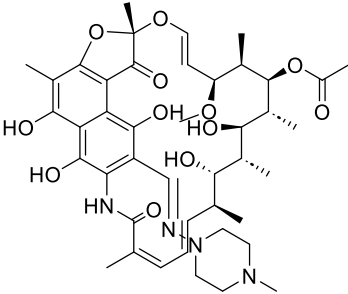
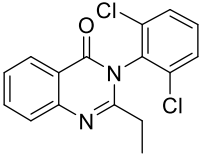
3.5 Quinazolinone-containing drugs in clinical use

Since quinazolinone skeleton-containing medications are widely recognized as a significant class of therapeutic drugs, many quinazolinone compounds have been developed and tested for a variety of biological activities. This quick progress suggests that other quinazolinone derivatives may soon be undergoing clinical trials. Methaqualone is the first well-known quinazolinone medication on the market and has been used since 1951 for sedative and hypnotic effects.[49] Many quinazolinone derivatives are currently patented and on the market as possible treatments for a range of illnesses. selected examples of commercially available quinazolinone medications for the treatment of different illnesses are shown in the following table (Table 3).

Gefitinib, erlotinib, vandetanib, trimetrexate, evodiamine, elinogrel, letermovir, milciclib, and sotrastaurin are other quinazolinone-containing marketed drugs.[50] [51]

Table 3: A summative table of selected quinazolinones containing drugs available in clinical use.

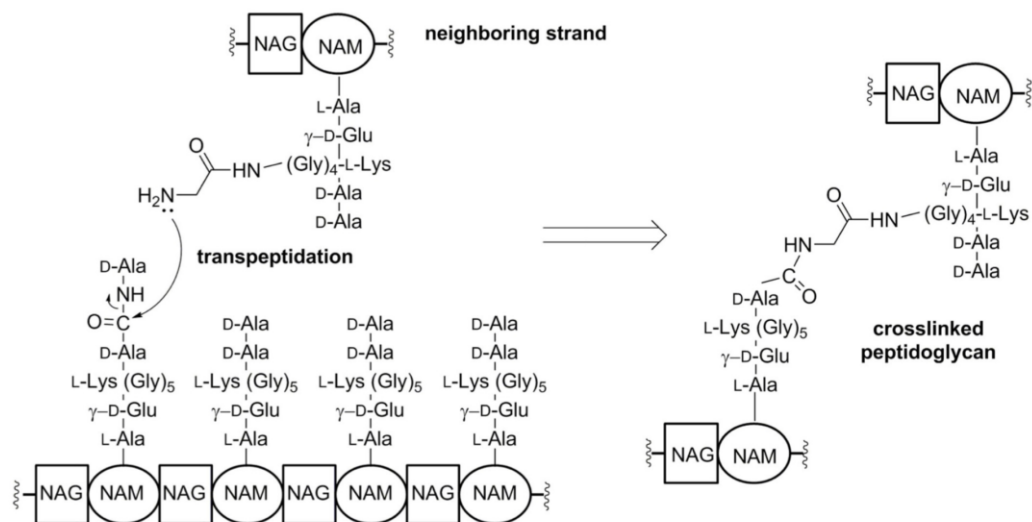
Drug	Structure	Activity	Target
Albaconazole [52] [53] [54]		Antifungal	Inhibits the synthesis of ergosterols by obstructing the 14- α -demethylase enzyme, leading to the accumulation of toxic methylsterols that could ultimately cause fungal death
Halofuginone [55] [56]		Coccidiostat, Antitumor, Autoimmune disorders	potent inhibitor of collagen α 1(I) and matrix metalloproteinase 2 (MMP-2) gene expression
Ispinesib [57–58]		Anticancer	inducing incomplete mitosis with nuclear disruption
Quinethazone [59] [60]		Antihypertensive, diuretic	inhibits Na^+/Cl^- reabsorption from the distal convoluted tubules in the kidneys
Proquazone [61]		Non-steroidal anti-inflammatory potential	inhibits the synthesis of prostaglandins by inhibiting cyclooxygenase

<p>Methaqualone [49] [62] [63]</p>		<p>Hypnotic</p>	<p>positive allosteric modulator at αGABA_A receptors</p>
<p>Afloqualone [64] [65]</p>		<p>Sedative, Hypnotic, Anticancer, Anxiolytic</p>	<p>agonist activity at the β subtype of the GABA_A receptor</p>
<p>Diproqualone [63]</p>		<p>Anxiolytic, Analgesic, Antihistamine, Rheumatoid Arthritis</p>	<p>agonist activity at the β subtype of the GABA_A receptor, antagonist activity at all histamine receptors, inhibition of the cyclooxygenase-1 enzyme</p>
<p>Etaqualone [62] [63]</p>	 <p>rifampicin</p>	<p>Sedative, hypnotic, muscle relaxant, and central nervous system depressant characteristics</p>	<p>positive allosteric modulator at human α1,2,3,5β2,3γ2S GABA_A receptors</p>
<p>Cloroqualone [63]</p>		<p>Sedative, hypnotic, cough suppressant</p>	<p>positive allosteric modulator at αGABA_A receptors</p>

3.6. Design rationale of thesis work

SA relies on the integrity of their cell walls to survive. SA uses the peptidoglycan as their primary building block to biosynthesize their cell wall. Repeats of the disaccharide *N*-acetylglucosamine (NAG)-*N*-acetylmuramic acid (NAM) with peptide stems on the NAM

unit build up the peptidoglycan. The sites of crosslinking that produce the mature cell wall are the peptide stems of nearby peptidoglycan strands.[66–67] (Fig. 5) Penicillin-binding proteins (PBPs), also known as transpeptidases, catalyze the crosslinking reaction during the synthesis of the peptidoglycan backbone. Transglycosylases carry out this catalytic role. The complex procedure of coordinating these reactions yields the construction of the cell wall.[68–69] β -lactam antibiotics, in particular, have a preference for targeting PBPs since their action is critical to bacterial survival. There are four native PBPs in *S. aureus*: PBP1, PBP2, PBP3, and PBP4. PBP2a is the fifth PBP found in MRSA. It is the resistance determinant in MRSA that was previously mentioned. Tipper and Strominger stated that because the β -lactam backbone is identical to the acyl-D-Ala- D-Ala segment of the peptide stem in the peptidoglycan, the physiological substrate of PBPs, PBPs are able to recognize and are effectively inhibited by β -lactam antibiotics (Fig. 6).[70] Because PBP2a is a special transpeptidase, β -lactam antibiotics do not effectively block it.[15] As a result, researchers are able to create novel antibiotics that are active against PBP2a, such as derivatives of quinazolinone.



Crosslinking of peptidoglycan strands in cell-wall synthesis. Elongation of the glycan strand is carried out by PBPs with transglycosylase activity. The transpeptidation reaction, where the terminal D-Ala is displaced and the peptide stems are crosslinked is accomplished by PBPs such as PBP2a in MRSA.

Figure 5: Crosslinking of peptidoglycan in cell wall synthesis. Elongation of glycan strands are carried out by PBPs with transglycosylase activity. This figure was taken without modification from [15]

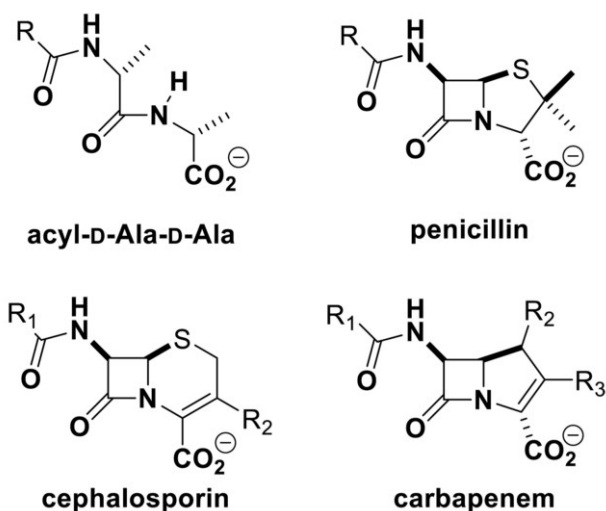


Figure 6: The core structures of penicillins, cephalosporins, and carbapenems mimic the d-Ala-d-Ala of the peptide stem of the cell wall. This figure was taken without modification from [15]

It was reported that the quinazolinone and β -lactam antibiotics have synergistic activity.[71] Commercial piperacillin-tazobactam and quinazolinone together demonstrated bactericidal synergy at sub-MICs for all three medications. The triple-drug combination's effectiveness was shown in a mouse model of MRSA neutropenic thigh infection. According to the theory underlying the antistaphylococcal synergistic effect, tazobactam inhibits the deactivating β -lactamase, and piperacillin inhibits PBP 2. In addition, quinazolinone binds to PBP 2a's allosteric site, inducing the allosteric response. As a result, the active site opens and binds to another piperacillin molecule. In other words, quinazolinone makes PBP 2a, which is typically not inhibited by piperacillin, more susceptible to inhibition. Authors provided crystal structures for complexes of the antibiotics with PBP 2a (refer to Figure 7) that supports the proposed mechanism of action.[71]

Table 4: MIC values of quinazolinone compound and vancomycin (VAN) against a panel of *Staphylococcus aureus* strains. The table was adapted from [71]

Strain	HA/CA	SCC type	MIC ($\mu\text{g}/\text{mL}$)	
			Compound 2	VAN
VRS4 ^b	HA	IV	0.25	64
NRS22 ^c	HA	II	0.25	8
NRS386	HA/CA	IV	0.125	1
NRS387	Pediatric	IV	0.125	1
NRS483	CA	IV	0.25	1
NRS484	CA	IV	0.125	1
NRS714	HA	IV	0.125	2
NRS249	HA	IV	0.125	2
NRS70	HA	II	0.25	1
NRS123	CA	IV	0.125	2
VRS1 ^b	HA	II	1	64
VRS2 ^b	HA	II	0.25	32
NRS384	CA	IV	0.03	1
NRS100		I	0.25	2
NRS119 ^d	HA	IV	0.125	1
ATCC 29213 ^{e,f}			0.03	1
NRS72 ^{e,g}			0.06	1
NRS77 ^h			0.125	1
NRS112 ^{e,i}			0.03	1
NRS128 ^{e,j}			0.5	1

^aCA, community acquired; HA, hospital acquired; SCC, staphylococcal cassette chromosome.

^bVancomycin-resistant strain.

^cHeteroVISA strain. The strain was deposited as a heterogeneous vancomycin-intermediate *S. aureus* phenotype. VISA strains show an MIC of 4 to 8 $\mu\text{g}/\text{mol}$ for vancomycin.

^dLinezolid-resistant strain (MIC of linezolid, 32 $\mu\text{g}/\text{mL}$).

^e β -Lactamase-positive MSSA strain.

^fMSSA standard quality control strain used in the laboratory.

^gMSSA476; hypervirulent and community acquired; USA400.

^hMSSA (RN1); derived from NCTC8325; *blaZ* negative.

ⁱMSSA (MN8); high-density pathogenic variant.

^jMSSA derived from NCTC8325; *blaZ* positive.

Note: vancomycin's MICs were 1 to 64 $\mu\text{g}/\text{ml}$, while quinazolinone's ranged from 0.03 to 1 $\mu\text{g}/\text{ml}$.

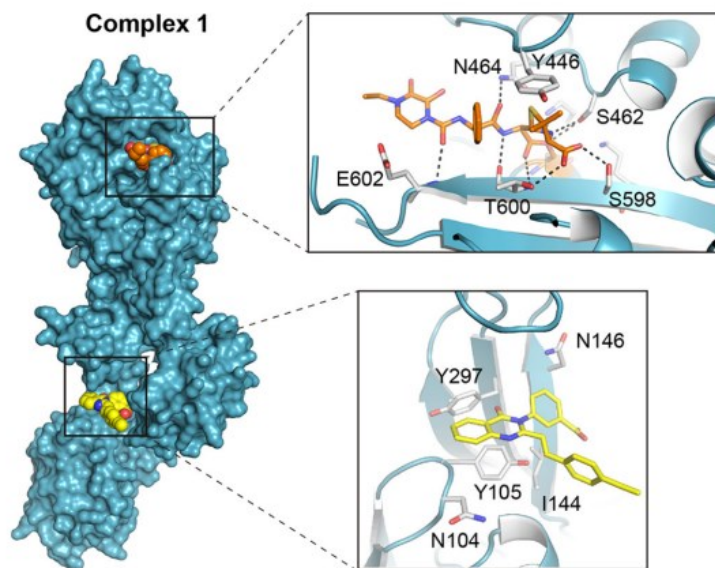


Figure 7: The ternary complex of PBP 2a-quinazolinone-piperacilin (PIP)) in three dimensions. The molecular surface of the complex is displayed, with quinazolinone and PIP represented by spheres (the carbon atoms are orange and yellow, respectively). The residues' interactions with ligands at the allosteric and active sites are shown in detail. The dotted lines are used to illustrate polar interactions. Taken from: [71]

Ghada Bouz, Ph.D. and Marek Kerda, colleagues in our research group, created the basic general structure shown in figure 8 below based on the SARs of antistaphylococcal quinazolinones targeting bacterial PBP 2a. Following that, they carried out in silico docking into the targeted SA PBP 2a enzyme's active region (PDB ID: 6Q9N), where we discovered typical intermolecular hydrogen bonding. Based on an in silico docking study, this work is a component of a wider series of molecules. The linkers, methylene (the primary subject of this diploma project), imine, carbonyl, and urea, are what distinguish them from one another.

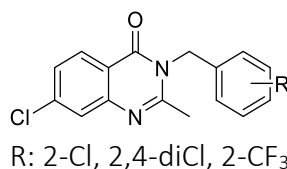


Figure 8: The basic structure of the compounds in this diploma study

The antistaphylococcal activity of each final product was assessed, and as a supplementary test, they were screened for antimycobacterial activity against

M. tuberculosis H37Rv, *M. kansasii*, *M. avium*, *M. tuberculosis H37Ra*, *M. smegmatis* and *M. aurum*, antibacterial activity against *Enterococcus faecalis*, *Escherichia coli*, *Klebsiella pneumoniae*, *Serratia marcescens* and *Pseudomonas aeruginosa* and antifungal activity against *Candida albicans*, *Candida krusei*, *Candida tropicalis*, *Candida parapsilosis*, *Aspergillus fumigatus*, *Aspergillus flavus*, *Lichtheimia corymbifera* and *Trichophyton interdigitale*. Throughout the text, compounds have been organized in ascending order according to their determined lipophilicity (log P value).

4. EXPERIMENTAL PART

4.1. Instrumentation

Without being further purified, all reagents and solvents (unless otherwise indicated) have been purchased from Sigma-Aldrich in Schnelldorf, Germany.

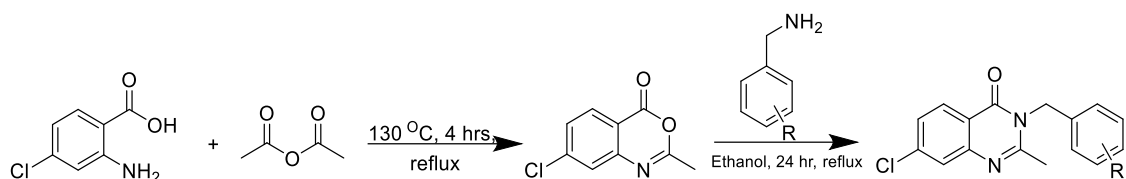
The majority of the chemical reactions took place at room temperature and in standard laboratory glassware. Thin Layer Chromatography (TLC) with UV detection at a wavelength of 254 nm (Alugram® Sil G/UV254, Machery-Nagel, Postfach, Germany) was used to monitor the reaction's development. For selected compounds, microwave-assisted reactions were carried out in a CEM Discover microwave reactor with a focused field (CEM Corporation, Matthews, NC, USA) connected to an Explorer 24 autosampler (CEM Corporation). The resulting compounds were subjected to flash chromatography using a puriFlash XS420+ (Interchim, Montluçon, France) equipped with original columns (spherical silica, 30 µm) supplied by the same company. The mobile phase was ethyl acetate (EtOAc) in hexane (Hex), gradient elution 0–100%, and detection took place by UV-VIS detector at 254 nm and 280 nm. NMR spectra of prepared compounds were recorded on Jeol JNM-ECZ600 (JEOL, Tokyo, Japan) at 600 MHz for ^1H and 151 MHz for ^{13}C . The chemical shifts were indirectly referenced to tetramethylsilane (TMS) via the solvent signal (2.49 ppm for ^1H and 39.70 ppm for ^{13}C in $\text{DMSO-}d_6$ and 7.26 for ^1H and 77.0 for ^{13}C in CDCl_3). Infrared spectra were recorded with spectrometer FT-IR Nicolet 6700 (Thermo Scientific, Waltham, MA, USA) using attenuated total reflectance (ATR-Ge) methodology. Elemental analysis will be carried out using a vario Micro Cube Elemental Analyzer (Elementar Analysensysteme GmbH, Hanau, Germany). Melting points were evaluated by SMP30 Stuart Scientific (Bibby Sterling Ltd., Staffordshire, UK) in open capillary. ChemDraw Professional 22.2 (CambridgeSoft, Cambridge, MA, USA) was used to determine the lipophilicity parameter log P.

4.2. Chemistry

4.2.1. General procedure

The general procedure is depicted in Scheme 1.

The starting material was prepared by reacting 3.6 g; (36 mmol) of 2-amino-4-chlorobenzoic acid with 50 mL of acetic anhydride under the reflux at 130 °C for four hours. Then, the liquids were evaporated under reduced pressure for thirty minutes. The obtained solid crude product was recrystallized from hexane 500 mL and ethyl acetate (EtOAc) 5 mL. After crystallization process, product crystals were filtered by Buchner funnel to obtain final product which was the starting material for the final reactions. Final products were prepared by reacting starting material (585 mg; 3 mmol) with corresponding substituted chlorinated benzylamine (1.2 eq) in 10 mL of ethanol as solvent under reflux (80 °C) for 24 hours. This is a typical aminolysis reaction in which an amine and a lactone combine to generate a lactam. Reaction was stopped and reaction mixture was checked by TLC using hexane: EtOAc 2:1 mobile phase system. Following the addition of 30 mL of EtOAc to dilute the reaction, 30 mL of acidic distilled water (water containing 10% HCl) was added. After thoroughly combining the two phases at room temperature using a magnetic stirrer, they were moved to a 250 mL separating funnel. The two layers were then allowed to settle and were separated into two 250 mL beakers. The aqueous layer was rewash with EtOAc (2 X 30 mL). Following each extraction, the combined organic layers were cleaned using 30 mL of brine and 100 mL of distilled water. The final organic layer was then moved to a 150 mL beaker (or less, depending on the total volume that was achieved) and allowed to sit at room temperature for 10 minutes while being agitated with magnesium sulfate (4 mmol, 500 mg) acting as a desiccant. The dispersion was then filtered through cotton, and the filtrate was then adsorbed to silica gel and purified using gradient elution 0 to 100% EtOAc in hexane in flash chromatography. The final product was transferred to a flask for evaporation and after this step approximately 19 mg of final product was sent for NMR spectroscopy.

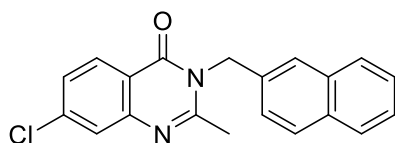


Scheme 1. General synthetic scheme of the title compounds.

Table 5: Exact quantities used of reactant 1 (7-chloro-2-methyl-4*H*-benzo[*d*][1,3]-oxazin-4-one) and reactant 2 (corresponding benzyl amine), with the yield of final compounds.

Code of the final compound	Reactant 1		Reactant 2			Isolated yield	
	n (mmol)	m (mg)	R	n (mmol)	m (mg)	m (mg)	% to theoretical
GDM18	3	585	4-OH	3.6	443.3	470	52
GDM29	4	780	2,4-diMeO	4.8	802.6	230	16
GDM32	3	585	3-MeO	3.6	493.8	250	26
GDM31	3	585	4-MeO	3.6	493.8	250	26
GDM20	3	585	2-F	3.6	450.5	220	24
GDM22	3	585	4-F	3.6	450.5	200	22
GDM30	2	390	2-Me	2.4	290.8	260	43
GDM27	3	585	3-Cl	3.6	509.7	240	25
GDM24	3	585	4-CF ₃	3.6	630.5	239	22
GDM35*	3	585	*	3.6	566	350	34
GDM26	3	585	3,4-diCl	3.6	633.7	275	30

* The structure of GDM35 is

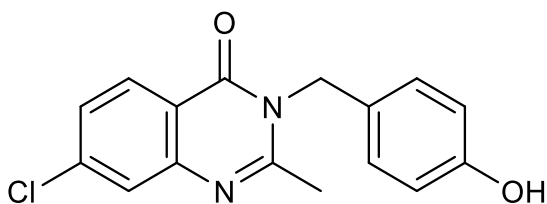


4.2.2. Final compounds

Smiles of Final Compounds

Code	Smiles
GDM18	<chem>ClC1=CC(N=C2C)=C(C=C1)C(N2CC3=CC=C(O)C=C3)=O</chem>
GDM29	<chem>ClC1=CC(N=C2C)=C(C=C1)C(N2CC3=CC=C(OC)C=C3OC)=O</chem>
GDM32	<chem>ClC1=CC(N=C2C)=C(C=C1)C(N2CC3=CC=CC(OC)=C3)=O</chem>
GDM31	<chem>ClC1=CC(N=C2C)=C(C=C1)C(N2CC3=CC=C(OC)C=C3)=O</chem>
GDM20	<chem>ClC1=CC(N=C2C)=C(C=C1)C(N2CC3=CC=CC=C3F)=O</chem>
GDM22	<chem>ClC1=CC(N=C2C)=C(C=C1)C(N2CC3=CC=C(F)C=C3)=O</chem>
GDM30	<chem>ClC1=CC(N=C2C)=C(C=C1)C(N2CC3=CC=CC=C3C)=O</chem>
GDM27	<chem>ClC1=CC(N=C2C)=C(C=C1)C(N2CC3=CC=CC(Cl)=C3)=O</chem>
GDM24	<chem>ClC1=CC(N=C2C)=C(C=C1)C(N2CC3=CC=C(C(F)(F)F)C=C3)=O</chem>
GDM35	<chem>ClC1=CC(N=C2C)=C(C=C1)C(N2CC3=CC(C=CC=C4)=C4C=C3)=O</chem>
GDM26	<chem>ClC1=CC(N=C2C)=C(C=C1)C(N2CC3=CC=C(Cl)C(Cl)=C3)=O</chem>

Code: GDM18



Chemical Name: 7-chloro-3-(4-hydroxybenzyl)-2-methylquinazolin-4(3H)-one

Chemical Formula: C₁₆H₁₃ClN₂O₂

Molecular weight: 300.74 g/mol

Log P: 3.11

Yield: 52%

Appearance: dark beige powder

m.p.: 178–179 °C

R_f (Hexane/EtOAc 2:1): 0.4

¹H NMR (600 MHz, DMSO-*d*₆) δ 9.37 (s, 1H), 8.09 (d, *J* = 8.5 Hz, 1H), 7.61 (d, *J* = 2.0 Hz, 1H), 7.51 – 7.46 (m, 1H), 7.03 – 6.98 (m, 2H), 6.71 – 6.66 (m, 2H), 5.20 (s, 2H, CH₂), 2.06 (s, 3H, CH₃).

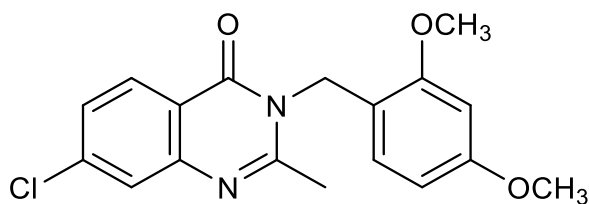
¹³C NMR (151 MHz, DMSO-*D*₆) δ 161.50, 157.47, 157.25, 148.70, 140.92, 139.59, 129.26, 129.09, 128.50, 127.22, 126.84, 126.26, 116.06, 115.62, 46.56, 23.56.

IR: (ATR-Ge, cm⁻¹) 3293 (N–H stretch), 2910 (C–H stretch), 1677 (C=O carbonyl stretch), 1621, 1590 (C–C aromatic stretch).

Elemental analysis: Calculated: 63.90% C; 4.36% H; 11.79% Cl, 9.31% N.

Found: 63.82% C; 4.44% H; 11.89% Cl, 9.45% N.

Code: GDM29



Chemical Name: 7-chloro-3-(2,4-dimethoxybenzyl)-2-methylquinazolin-4(3H)-one

Chemical Formula: C₁₈H₁₇ClN₂O₃

Molecular weight: 344.79 g/mol

Log P: 3.25

Yield: 16%

Appearance: yellow powder

m.p.: 175–177 °C

R_f (Hexane/EtOAc 2:1): 0.4

¹H NMR (600 MHz, DMSO-*d*₆) δ 8.07 (d, *J* = 8.6 Hz, 1H), 7.64 (d, *J* = 2.1 Hz, 1H), 7.52 – 7.47 (m, 1H), 6.63 (d, *J* = 8.4 Hz, 1H), 6.58 (d, *J* = 2.4 Hz, 1H), 6.41 – 6.36 (m, 1H), 5.13 (s, 2H, CH₂), 3.80 (s, 3H, OCH₃), 3.69 (s, 3H, OCH₃), 2.43 (s, 3H, CH₃).

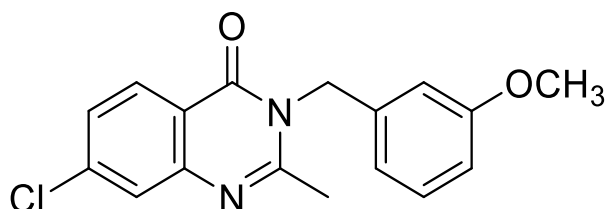
¹³C NMR (151 MHz, DMSO-*d*₆) δ 161.38, 160.47, 157.88, 157.58, 148.75, 139.59, 129.01, 127.23, 126.28, 119.28, 116.17, 105.46, 99.09, 56.13, 55.76, 42.56, 23.18.

IR: not enough compound.

Elemental analysis: Calculated: 62.70% C; 4.97% H; 10.28% Cl, 8.12% N.

Found: 62.75% C; 4.92% H; 10.17% Cl, 8.13% N.

Code: GDM32



Chemical Name: 7-chloro-3-(3-methoxybenzyl)-2-methylquinazolin-4(3H)-one

Chemical Formula: C₁₇H₁₅ClN₂O₂

Molecular weight: 314.77 g/mol

Log P: 3.38

Yield: 26%

Appearance: yellow powder

m.p.: 170–171 °C

R_f (Hexane/EtOAc 2:1): 0.4

¹H NMR (600 MHz, DMSO-*d*₆) δ 8.10 (d, *J* = 8.6 Hz, 1H), 7.78 (d, *J* = 8.4 Hz, 1H), 7.64 (d, *J* = 2.1 Hz, 1H), 7.53 – 7.48 (m, 1H), 7.24 – 7.17 (m, 3H), 5.30 (s, 2H, CH₂), 3.70 (s, 3H, OCH₃), 2.06 (s, 3H, CH₃).

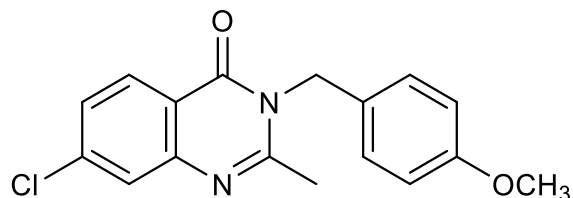
¹³C NMR (151 MHz, DMSO-*D*₆) δ 161.48, 157.43, 148.73, 141.03, 139.69, 136.90, 130.55, 129.99, 129.13, 126.34, 122.87, 120.25, 118.68, 113.55, 55.59, 46.92, 23.54.

IR: (ATR-Ge, cm⁻¹) 3361 (N–H stretch), 2922 (C–H stretch), 1674 (C=O carbonyl stretch), 1600, 1577 (C–C aromatic stretch).

Elemental analysis: Calculated: 64.87% C; 4.80% H; 11.26% Cl, 8.90% N.

Found: 64.78% C; 4.89% H; 11.37% Cl, 8.89% N.

Code: GDM31



Chemical Name: 7-chloro-3-(4-methoxybenzyl)-2-methylquinazolin-4(3H)-one

Chemical Formula: C₁₇H₁₅ClN₂O₂

Molecular weight: 314.77 g/mol

Log P: 3.38

Yield: 26%

Appearance: light beige powder

m.p.: 172–173 °C

R_f (Hexane/EtOAc 2:1): 0.4

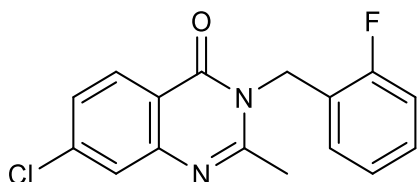
¹H NMR (600 MHz, CDCl₃) δ 8.20 (d, *J* = 8.5 Hz, 1H), 7.60 (d, *J* = 2.0 Hz, 1H), 7.41 – 7.38 (m, 1H), 7.16 – 7.10 (m, 2H), 6.91 – 6.81 (m, 2H), 5.29 (s, 2H, CH₂), 3.76 (s, 3H, OCH₃), 2.54 (s, 3H, CH₃).

¹³C NMR (151 MHz, CDCl₃) δ 161.96, 159.31, 156.12, 148.40, 140.62, 129.39, 128.68, 128.18, 127.73, 127.22, 126.43, 114.47, 55.39, 46.88, 23.60.

IR: (ATR-Ge, cm⁻¹) 3325 (N–H stretch), 2960 (C–H stretch), 1674 (C=O carbonyl stretch), 1603, 1585, 1564 (C–C aromatic stretch).

Elemental analysis: Calculated: 64.87% C; 4.80% H; 11.26% Cl, 8.90% N.
Found: 64.76% C; 4.91% H; 11.25% Cl, 8.80% N.

Code: GDM20



Chemical Name: 7-chloro-3-(2-fluorobenzyl)-2-methylquinazolin-4(3H)-one

Chemical Formula: C₁₆H₁₂ClFN₂O

Molecular weight: 302.73 g/mol

Log P: 3.66

Yield: 24%

Appearance: light beige powder

m.p.: 168–169 °C

R_f (Hexane/EtOAc 2:1): 0.5

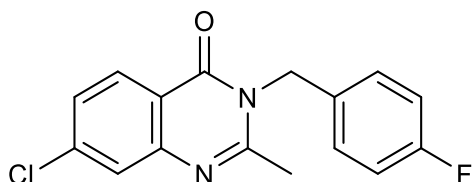
¹H NMR (600 MHz, DMSO-*d*₆) δ 8.07 (d, *J* = 8.5 Hz, 1H), 7.65 (d, *J* = 2.0 Hz, 1H), 7.52 – 7.47 (m, 1H), 7.34 – 7.28 (m, 1H), 7.25 – 7.19 (m, 1H), 7.10 (t, *J* = 7.5 Hz, 1H), 7.02 – 6.96 (m, 1H), 5.33 (s, 2H, CH₂), 2.48 (s, 3H, CH₃).

¹³C NMR (151 MHz, DMSO-*d*₆) δ 161.33, 159.45, 157.25, 148.71, 139.75, 130.00 (q, *J* = 32 Hz), 129.02, 128.18, 127.37, 126.36 (q, *J* = 272.4 Hz), 125.42, 123.56, 119.19 (q, *J* = 6 Hz), 116.14 (q, *J* = 4 Hz), 41.83, 23.33.

IR: (ATR-Ge, cm⁻¹) 3298 (N–H stretch), 2990 (C–H stretch), 1680 (C=O carbonyl stretch), 1601, 1564 (C–C aromatic stretch).

Elemental analysis: Calculated: 63.48% C; 4.80% H; 11.71% Cl, 9.25% N.

Code: GDM22



Chemical Name: 7-chloro-3-(4-fluorobenzyl)-2-methylquinazolin-4(3H)-one

Chemical Formula: C₁₆H₁₂ClFN₂O

Molecular weight: 302.73 g/mol

Log P: 3.66

Yield: 22%

Appearance: yellow powder

m.p.: 167–168 °C

R_f (Hexane/EtOAc 2:1): 0.5

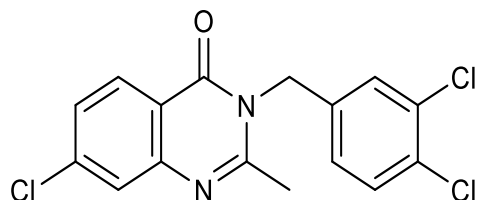
¹H NMR (600 MHz, DMSO-*d*₆) δ 8.09 (d, *J* = 8.5 Hz, 1H), 7.62 (d, *J* = 2.1 Hz, 1H), 7.51 – 7.47 (m, 1H), 7.27 – 7.21 (m, 2H), 7.21 – 7.09 (m, 2H), 5.30 (s, 2H, CH₂), 2.45 (s, 3H, CH₃).

¹³C NMR (151 MHz, DMSO-*d*₆) δ 162.75, 161.49, 157.29, 148.70, 139.69, 132.97 (q, *J* = 33 Hz), 132.95, 129.19, 129.07, 127.30, 126.31 (q, *J* = 272.2 Hz), 119.27, 116.19 (q, *J* = 5 Hz), 116.05 (q, *J* = 4 Hz), 46.46, 23.57.

IR: (ATR-Ge, cm⁻¹) 3283 (N–H stretch), 2956 (C–H stretch), 1672 (C=O carbonyl stretch), 1601, 1592 (C–C aromatic stretch).

Elemental analysis: Calculated: 63.48% C; 4.80% H; 11.71% Cl, 9.25% N.

Code: GDM30



Chemical Name: 7-chloro-2-methyl-3-(2-methylbenzyl)quinazolin-4(3H)-one

Chemical Formula: C₁₇H₁₅ClN₂O

Molecular weight: 298.77 g/mol

Log P: 3.99

Yield: 43%

Appearance: yellow powder

m.p.: 168–170 °C

R_f (Hexane/EtOAc 2:1): 0.5

¹H NMR (600 MHz, CDCl₃) δ 8.21 (d, *J* = 8.3 Hz, 1H), 7.65 (d, *J* = 2.0 Hz, 1H), 7.44 – 7.39 (m, 1H), 7.25 (s, 1H), 7.24 – 7.12 (m, 1H), 7.11 – 7.05 (m, 1H), 6.64 (d, *J* = 7.4 Hz, 1H), 5.31 (s, 2H, CH₂), 2.47 (s, 3H, CH₃), 2.41 (s, 3H, CH₃).

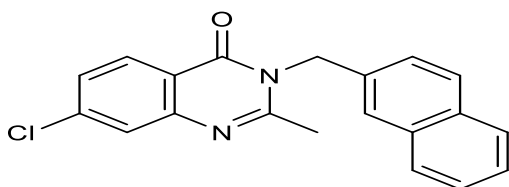
¹³C NMR (151 MHz, DMSO-*d*₆) δ 161.42, 158.31, 157.49, 148.73, 139.71, 138.15, 130.43, 129.12, 127.34, 126.34, 119.20, 117.39, 114.91, 113.31, 46.81, 40.61, 23.49.

IR: (ATR-Ge, cm⁻¹) 3375 (N–H stretch), 2943 (C–H stretch), 1682 (C=O carbonyl stretch), 1629, 1593, 1562 (C–C aromatic stretch).

Elemental analysis: Calculated: 68.34% C; 5.06% H; 11.87% Cl, 9.38% N.

Found: 68.25% C; 5.15% H; 11.98% Cl, 9.37% N.

Code: GDM27



Chemical Name: 7-chloro-3-(3-chlorobenzyl)-2-methylquinazolin-4(3*H*)-one

Chemical Formula: C₁₆H₁₂Cl₂N₂O

Molecular weight: 319.19 g/mol

Log *P*: 3.99

Yield: 25%

Appearance: light yellow powder

m.p.: 165–166 °C

R_f (Hexane/EtOAc 2:1): 0.4

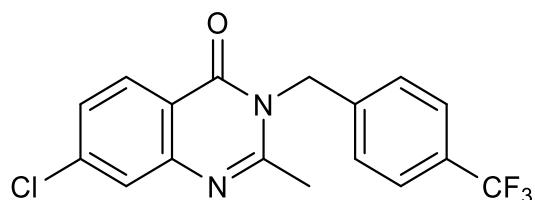
¹H NMR (600 MHz, CDCl₃) δ 8.21 (d, *J* = 8.5 Hz, 1H), 7.62 (d, *J* = 2.0 Hz, 1H), 7.44 – 7.38 (m, 1H), 7.30 – 7.22 (m, 2H), 7.19 – 7.13 (m, 1H), 7.09 – 7.03 (m, 1H), 5.33 (s, 2H, CH₂), 2.52 (s, 3H, CH₃).

¹³C NMR (151 MHz, CDCl₃) δ 161.82, 155.69, 148.37, 140.88, 137.75, 135.14, 130.42, 128.71, 128.25, 127.45, 126.79, 126.58, 124.76, 118.84, 46.82, 23.57.

IR: (ATR-Ge, cm⁻¹) 3388 (N–H stretch), 2967 (C–H stretch), 1673 (C=O carbonyl stretch), 1621, 1592 (C–C aromatic stretch).

Elemental analysis: Calculated: 60.21% C; 3.79% H; 22.21% Cl, 8.78% N.
Found: 60.32% C; 3.68% H; 22.22% Cl, 8.67% N.

Code: GDM24



Chemical Name: 7-chloro-2-methyl-3-(4-(trifluoromethyl)benzyl)quinazolin-4(3H)-one

Chemical Formula: C₁₇H₁₂ClF₃N₂O

Molecular weight: 352.74 g/mol

Log P: 4.42

Yield: 22%

Appearance: Yellow powder

m.p.: 171–172 °C

R_f (Hexane/EtOAc 2:1): 0.5

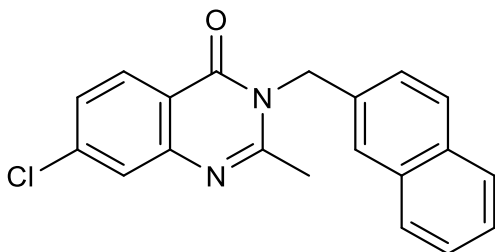
¹H NMR (600 MHz, CDCl₃) δ 8.20 (d, *J* = 8.5 Hz, 1H), 7.65 – 7.56 (m, 2H), 7.46 – 7.37 (m, 2H), 7.32 – 7.27 (m, 2H), 5.40 (s, 2H, CH₂), 2.52 (s, 3H, CH₃).

¹³C NMR: not enough sample.

IR: (ATR-Ge, cm⁻¹) 3366 (N–H stretch), 2940 (C–H stretch), 1681 (C=O carbonyl stretch), 1645, 1608, 1588 (C–C aromatic stretch).

Elemental analysis: Calculated: 57.89% C; 3.43% H; 10.05% Cl, 7.94% N.

Code: GDM35



Chemical Name: 7-chloro-2-methyl-3-(naphthalen-2-ylmethyl)quinazolin-4(3H)-one

Chemical Formula: C₂₀H₁₅ClN₂O

Molecular weight: 334.80 g/mol

Log P: 4.5

Yield: 34%

Appearance: light yellow powder

m.p.: 175–176 °C

R_f (Hexane/EtOAc 2:1): 0.5

¹H NMR (600 MHz, CDCl₃) δ 8.23 (d, *J* = 8.6 Hz, 1H), 8.03 (d, *J* = 8.3 Hz, 1H), 7.91 (dd, *J* = 8.3, 1.4 Hz, 1H), 7.85 – 7.75 (m, 1H), 7.69 (d, *J* = 2.0 Hz, 1H), 7.64 – 7.59 (m, 1H), 7.59 – 7.53 (m, 1H), 7.48 – 7.38 (m, 1H), 7.36 – 7.30 (m, 1H), 6.85 – 6.79 (m, 1H), 5.83 (s, 2H, CH₂), 2.48 (s, 3H, CH₃).

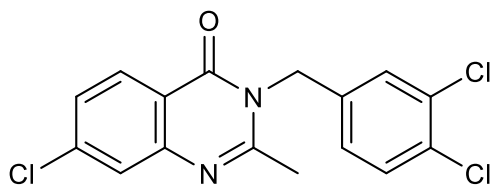
¹³C NMR (151 MHz, CDCl₃) δ 161.77, 156.40, 148.50, 140.83, 133.89, 130.47, 129.22, 128.79, 128.30, 127.41, 126.78, 126.55, 126.29, 125.61, 125.52, 122.15, 121.45, 118.84, 44.93, 23.21.

IR: (ATR-Ge, cm⁻¹) 3386 (N–H stretch), 2942 (C–H stretch), 1683 (C=O carbonyl stretch), 1589, 1561 (C–C aromatic stretch).

Elemental analysis: Calculated: 71.75% C; 4.52% H; 10.59% Cl, 8.37% N.

Found: 71.64% C; 4.61% H; 10.48% Cl, 8.38% N.

Code: GDM26



Chemical Name: 7-chloro-3-(3,4-dichlorobenzyl)-2-methylquinazolin-4(3H)-one

Chemical Formula: C₁₆H₁₁Cl₃N₂O

Molecular weight: 353.63 g/mol

Log P: 4.62

Yield: 30%

Appearance: light beige powder

m.p.: 170–172 °C

R_f (Hexane/EtOAc 2:1): 0.5

¹H NMR (600 MHz, CDCl₃) δ 8.64 (d, *J* = 2.1 Hz, 1H), 8.18 (d, *J* = 8.4 Hz, 1H), 7.62 (d, *J* = 2.0 Hz, 1H), 7.43 – 7.37 (m, 2H), 7.18 – 7.13 (m, 1H), 5.27 (s, 2H, CH₂), 2.17 (s, 3H, CH₃).

¹³C NMR (151 MHz, DMSO-*d*₆) δ 169.19, 168.06, 161.53, 157.16, 148.72, 138.03, 137.00, 131.45, 130.40, 129.34, 126.34, 122.92, 120.40, 119.29, 46.30, 23.63.

IR: (ATR-Ge, cm⁻¹) 3361 (N–H stretch), 2924 (C–H stretch), 1677 (C=O carbonyl stretch), 1599, 1581 (C–C aromatic stretch).

Elemental analysis: Calculated: 54.34% C; 3.14% H; 30.07% Cl, 7.92% N.

Found: 54.23% C; 3.25% H; 30.16% Cl, 7.71% N.

4.3. *Biological Assays*

4.3.1. *In Vitro* Antibacterial Activity Evaluation

Microdilution broth method was performed by Dr. Klára Konečná, Ida Dufková. and Jana Vacková from the group of microbiology and immunology at Faculty of Pharmacy in Hradec Kralove according to the procedure reported in the latest published article by our research group: [72] (“Antibacterial evaluation was performed against eight bacterial strains from the Czech Collection of Microorganisms (CCM, Brno, Czech Republic) (*Staphylococcus aureus* CCM 4223 (ATCC 29213), *Staphylococcus aureus* methicilin resistant CCM 4750 (ATCC 43300), *Enterococcus faecalis* CCM 4224 (ATCC 29212), *Escherichia coli* CCM 3954 (ATCC 25922), *Pseudomonas aeruginosa* CCM 3955 (ATCC 27853)) or clinical isolates from the Department of Clinical Microbiology, University Hospital and Faculty of Medicine in Hradec Králové, Charles University in Prague, Czech Republic (*Staphylococcus epidermidis* 112-2016, *Klebsiella pneumoniae* 64-2016, *Serratia marcescens* 62-2016). All strains were subcultured on Mueller-Hinton agar (MHA) (Difco/Becton Dickinson, Detroit, MI, USA) at 35 °C and maintained on the same medium at 4 °C. The compounds were dissolved in DMSO, and the antibacterial activity was determined in cation adjusted Mueller-Hinton liquid broth (Difco/Becton Dickinson) buffered to pH 7.0. Controls consisted of medium and DMSO solely. The final concentration of DMSO in the test medium did not exceed 1% (v/v) of the total solution composition. The minimum inhibitory concentration (MIC) was determined after 24 and 48 h of static incubation at 35 °C by visual inspection or using Alamar Blue dye. The standards were gentamicin and ciprofloxacin. All experiments were conducted in duplicate. For the results to be valid, the difference in MIC for one compound determined from two parallel measurements must not be greater than one step on the dilution scale.”)[72]

4.3.2. *In Vitro* Activity Evaluation Against *Mycobacterium tuberculosis*, *Mycobacterium kansasii*, and *Mycobacterium avium*

Microdilution panel method was performed by Pavla Paterová, Ph.D., at the Department of Clinical Microbiology, University Hospital Hradec Králové, according to the procedure reported in the latest published article by our research group: [72] (“Tested strains *M. tuberculosis* H37Rv CNCTC My 331/88 (ATCC 27294), *M. kansasii* Hauduroy CNCTC My 235/80 (ATCC 12478), *M. avium* ssp. *Avium* Chester CNCTC My 80/72 (ATCC 15769) were obtained from Czech National Collection of Type Cultures (CNCTC), National Institute of Public Health, Prague, Czech Republic. Middlebrook 7H9 broth (Sigma-Aldrich) enriched with 0.4% (v/v) of glycerol (Sigma-Aldrich) and 10% (v/v) of OADC supplement (oleic acid, albumin, dextrose, catalase; Himedia, Mumbai, India) of declared pH = 6.6. Tested compounds were dissolved and diluted in DMSO, mixed with broth (25 µL) of DMSO solution in 4.475 mL of broth and placed (100 µL) into microplate wells. Mycobacterial inocula were suspended in isotonic saline solution and the density was adjusted to 0.5–1.0 McFarland scale. These suspensions were diluted by 10^{-1} and used to inoculate the testing wells, adding 100 µL of mycobacterial suspension per well. Final concentrations of the tested compounds in wells were 100, 50, 25, 12.5, 6.25, 3.13, and 1.56 µg/mL.

INH and PZA were used as positive controls (inhibition of growth). Negative control (mycobacterial growth control) consisted of broth plus DMSO. Plates were statically incubated in a dark, humid atmosphere at 37 °C. After five days of incubation, 30 µL of Alamar Blue working solution (1:1 mixture of 0.01% resazurin sodium salt (aq. sol.) and 10% Tween 80) was added per well. Results were then determined after 24 h of incubation and interpreted according to Franzblau et al.²⁸. The minimum inhibition concentration (MIC, µg/mL) was determined as the lowest concentration that prevented the blue to pink colour change as indicated by visual inspection. The experiments were conducted in duplicates. For the results to be valid, the difference in MIC for one compound determined from two parallel measurements must not be greater than one step on the dilution scale.”)[72]

4.3.3. *In Vitro* Activity Evaluation Against *Mycobacterium smegmatis* and *Mycobacterium aurum*

Microdilution broth method was performed by Ondřej Jand'ourek, Ph.D. from the group of microbiology and immunology at Faculty of Pharmacy in Hradec Kralove according to the procedure reported in the latest published article by our research group: [72] ("Antimycobacterial assay was performed on fast growing *M. smegmatis* DSM 43465 (ATCC 607) and *M. aurum* DSM 43999 (ATCC 23366) from German Collection of Microorganisms and Cell Cultures (Braunschweig, Germany). The technique used for activity determination was microdilution broth panel method using 96-well microtitration plates. Culturing medium was Middlebrook 7H9 broth (Sigma-Aldrich) enriched with 0.4% of glycerol (Sigma-Aldrich) and 10% of Middlebrook OADC growth supplement (Himedia). Mycobacterial strains were cultured on Middlebrook 7H9 agar and suspensions were prepared in Middlebrook 7H9 broth. Final density was adjusted to value ranging from 0.5 to 1.0 according to McFarland scale and diluted in ratio 1:20 with broth. Tested compounds were dissolved in DMSO (Sigma-Aldrich) then MB broth was added to obtain concentration of 2000 µg/mL. Standards used for activity determination were INH, rifampicin (RIF) and ciprofloxacin (CPX) (Sigma-Aldrich). Final concentrations were reached by binary dilution and addition of mycobacterial suspension, and were set as 500, 250, 125, 62.5, 31.25, 15.625, 7.81, 3.91 µg/mL, except to standards rifampicin, where the final concentrations were 12.5, 6.25, 3.125, 1.56, 0.78, 0.39, 0.195, 0.098 µg/mL, and ciprofloxacin, where the final concentrations were 1, 0.5, 0.25, 0.125, 0.0625, 0.0313, 0.0156, 0.0078 µg/mL. The final concentration of DMSO did not exceeded 2.5% (v/v) and did not affect the growth of *M. smegmatis* or *M. aurum*. Positive (broth, DMSO, bacteria) and negative (broth, DMSO) controls were included. Plates were sealed with polyester adhesive film and incubated in dark at 37 °C without agitation. The addition of 0.01% solution of resazurin sodium salt followed after 48 h of incubation for *M. smegmatis*, and after 72 h of incubation for *M. aurum*. Stain was prepared by dissolving resazurin sodium salt (Sigma-Aldrich) in deionized water to get 0.02% solution. Then 10% aqueous solution of Tween 80 (Sigma-Aldrich) was prepared. Equal volumes of both liquids were mixed and filtered a through syringe membrane filter. Microtitration panels were then incubated for further 2.5 h for determination of activity against *M. smegmatis*, and 4 h for *M. aurum*. Antimycobacterial activity was expressed as minimal inhibition

concentration (MIC), and the value was read on the basis of stain colour change (blue colour—active compound; pink colour—inactive compound). MIC values for standards were in ranges 7.81–15.625 µg/mL for INH, 12.5–25 µg/mL for RIF, and 0.0625–0.125 µg/mL for CPX against *M. smegmatis*, 1.95–3.91 µg/mL for INH, 0.78–1.56 µg/mL for RIF, and 0.00781–0.01563 µg/mL for CPX against *M. aurum*, respectively. All experiments were conducted in duplicate. For the results to be valid, the difference in MIC for one compound determined from two parallel measurements must not be greater than one step on the dilution scale.”)[72]

4.3.4. *In Vitro* Antifungal Activity Evaluation

Antifungal evaluation was performed using a microdilution broth method by Dr. Klára Konečná, Ida Dufková. and Jana Vacková from the group of microbiology and immunology at Faculty of Pharmacy in Hradec Kralove according to the procedure reported in the latest published article by our research group: [72] (“against eight fungal strains from the Czech Collection of Microorganisms (CCM) (*Candida albicans* CCM 8320 (ATCC 24433), *C. krusei* CCM 8271 (ATCC 6258), *C. parapsilosis* CCM 8260 (ATCC 22019), *C. tropicalis* CCM 8264 (ATCC 750), *Aspergillus flavus* CCM 8363, *Lichtheimia corymbifera* CCM 8077 and *Trichophyton interdigitale* CCM 8377 (ATCC 9533) or from the American Type Collection Cultures (ATCC, Manassas, VA, USA) (*Aspergillus fumigatus* ATCC 204305). Compounds were dissolved in DMSO and diluted in a twofold manner with RPMI 1640 medium, with glutamine and 2% glucose, buffered to pH 7.0 (3-morpholinopropane-1-sulfonic acid). The final concentration of DMSO in the tested medium did not exceed 2.5% (v/v) of the total solution composition. Static incubation was performed in the dark and humid atmosphere, at 35 °C, for 24 and 48 h (72 and 120 h for *Trichophyton interdigitale* respectively). Drug-free controls were included. MIC was inspected visually or making use of Alamar Blue staining. The standards were amphotericin B and fluconazole. All experiments were conducted in duplicate. For the results to be valid, the difference in MIC for one compound determined from two parallel measurements must not be greater than one step on the dilution scale.”)[72]

4.4. Results and discussion

4.4.1. Chemistry

The final compounds were purified using flash chromatography, using ethyl acetate in hexane as an eluent. They were separated as solid, light-colored compounds with yields varying from 16 to 52% of products that were chromatographically pure.. The observed more or less low yields can be justified by the steric hindrance of the bicyclic structure of the 7-cholorenzoxazinones intermediates. We searched final compounds in the freely available tool ChemSpider provided by the Royal Society of Chemistry (RSC) (www.chemspider.com) for their reported ID and any detected biological evaluation/activity. A summary of the search results is provided in Table 6 below. There had been no prior reporting of any of the final compounds with ID or evaluated for biological activities. The novelty of our compounds is considered to be an advantage.

Table 6: Results of searching for title compounds in the literature using ChemSpider (www.chemspider.com)

Code	ChemSpider ID	Literature (RSC journals/PubMed)
GDM18	NA	NA
GDM29	NA	NA
GDM32	NA	NA
GDM31	NA	NA
GDM20	NA	NA
GDM22	NA	NA
GDM30	NA	NA
GDM27	NA	NA
GDM24	NA	NA
GDM35	NA	NA
GDM26	NA	NA

Note: NA = not available.

4.4.2. Predicted pharmacokinetics, drug-likeness, and medicinal chemistry features

We assessed our title compounds' pharmacokinetics, drug-likeness, and medicinal chemistry friendliness using the free online tool SwissADME (<http://www.swissadme.ch/index.php>).[73] Those characteristics that we considered most relevant are listed in tables 7-9 below.

Table 7: Selected descriptors and physicochemical properties of final compounds predicted using SwissADME tool.

Code	Num. heavy atoms	Num. rotatable bonds	Num. H-bond acceptors	Num. H-bond donors	Molar Refractivity	Topological Polar Surface Area (TPSA)
GDM18	21	2	3	1	83.75	55.12 Å ²
GDM29	24	4	4	0	94.71	53.35 Å ²
GDM32	22	3	3	0	88.22	44.12 Å ²
GDM31	22	3	3	0	88.22	44.12 Å ²
GDM20	21	2	3	0	81.69	34.89 Å ²
GDM22	21	2	3	0	81.69	34.89 Å ²
GDM30	21	2	2	0	86.69	34.89 Å ²
GDM27	21	2	2	0	86.74	34.89 Å ²
GDM24	24	3	5	0	86.73	34.89 Å ²
GDM35	24	2	2	0	99.23	34.89 Å ²
GDM26	22	2	2	0	91.75	34.89 Å ²

Table 8: The Pharmacokinetics properties of final compounds predicted using SwissADME tool.

Code	GI absorption	BBB permeant	P-gp substrate	CYP1A2 inhibitor	CYP3A4 inhibitor	Log Kp (skin permeation) in cm/s
GDM18	High	Yes	No	Yes	No	-6.26 cm/s
GDM29	High	Yes	No	Yes	Yes	-6.32 cm/s
GDM32	High	Yes	No	Yes	No	-6.11 cm/s
GDM31	High	Yes	No	Yes	No	-6.11 cm/s
GDM20	High	Yes	No	Yes	No	-5.95 cm/s
GDM22	High	Yes	No	Yes	No	-5.95 cm/s
GDM30	High	Yes	No	Yes	No	-5.74 cm/s
GDM27	High	Yes	No	Yes	No	-5.68 cm/s
GDM24	High	Yes	No	Yes	No	-5.70 cm/s
GDM35	High	Yes	No	Yes	No	-5.32 cm/s
GDM26	High	Yes	No	Yes	No	-5.44 cm/s

Table 9: The druglikeness and medicinal chemistry properties of final compounds predicted using SwissADME tool.

Code	Lipinski	Bioavailability Score	Pan Assay Interference Structure (PAINS)	XLOGP3	MLOGP	Leadlikeness
GDM18	Yes; 0 violation	0.55	0 alert	2.64	3.06	Yes
GDM29	Yes; 0 violation	0.55	0 alert	2.94	2.97	Yes
GDM32	Yes; 0 violation	0.55	0 alert	2.97	3.30	Yes
GDM31	Yes; 0 violation	0.55	0 alert	2.97	3.30	Yes
GDM20	Yes; 0 violation	0.55	0 alert	3.10	4.03	Yes
GDM22	Yes; 0 violation	0.55	0 alert	3.10	4.03	Yes
GDM30	Yes; 0 violation	0.55	0 alert	3.36	3.88	Yes
GDM27	Yes; 0 violation	0.55	0 alert	3.62	4.15	No; 1 violation: XLOGP3>3.5
GDM24	Yes; 1 violation: MLOGP>4.15	0.55	0 alert	3.88	4.49	No; 2 violations: MW>350, XLOGP3>3.5
GDM35	Yes; 1 violation: MLOGP>4.15	0.55	0 alert	4.25	4.38	No; 1 violation: XLOGP3>3.5
GDM26	Yes; 1 violation: MLOGP>4.15	0.55	0 alert	4.25	4.65	No; 2 violations: MW>350, XLOGP3>3.5

The pharmacokinetics and general druglikeness of a substance are significantly influenced by its physicochemical properties, which makes them crucial. Greater chemical complexity can impact a compound's metabolism and overall drug-likeness. [73] [74] This is particularly true for compounds with a higher number of heavy atoms (non-hydrogen atoms). Drug development may be more difficult for compounds with a higher number of heavy atoms because of possible problems with metabolism and excretion. Conversely, compounds with fewer heavy atoms are often smaller and may have superior drug-like qualities. In general, 20–50 heavy atoms are considered to be optimal for drug discovery.[75] All our compounds have heavy atom counts that fall within this favorable range. Solubility and membrane permeability are impacted by the quantity of hydrogen

bond donors and acceptors. We found that our compounds exhibit acceptable outcomes when compared to Lipinski's rule of five, which states that a good medication candidate (for peroral systemic application) typically includes no more than five hydrogen bond donors and ten hydrogen bond acceptors. Rotatable bonds influence molecule's flexibility; for optimal oral bioavailability, fewer rotatable bonds—less than ten—are generally preferable.[73] Molar refractivity may affect compound's solubility, pharmacokinetic profile overall, and how it interacts with its target. The drug's interaction with its biological target can be improved by a well-balanced molar refractivity without compromising permeability or solubility. For drug-like compounds, the average range of molar refractivity values is 40–130 cm³/mol. This range is wide enough to accommodate the diversity of molecule sizes and polarizabilities present in pharmaceuticals. Title compounds again fall within this favorable range. Topological polar surface area (TPSA) forecasts the compounds' absorption and distribution characteristics along with information about the compound's ability to pass through cell membranes. In general, improved permeability is indicated by a reduced TPSA (below 140 Å²), which is the case for our compounds. While these properties align well with established drug-likeness criteria, moderate solubility may require further optimization. Overall, compounds show promise as drug candidates, but *in vitro* and *in vivo* studies are necessary to confirm these computational predictions and to further assess their pharmacokinetic and metabolic profiles. [74]

SwissADME pharmacokinetic prediction, in summary, showed that the compounds have strong oral bioavailability with a risk of central nervous system side effects. They also have high gastrointestinal absorption, penetrate the blood-brain barrier, and are not P-glycoprotein substrates. Nevertheless, given that they are CYP1A2 inhibitors, there may be a chance for drug-drug interactions, which needs to be investigated more. The compounds have good skin penetration and could be beneficial for the treatment of skin infections, however more research would be needed to confirm this. In general, the compounds show encouraging pharmacokinetic characteristics, which could lead to their acceptance as candidates for additional drug development, provided that these predictions are validated through experimentation.[76] [77] [78]

Compounds (GDM22, GDM30, GDM27, GDM20, GDM29, GDM31, GDM18, and GDM32) analyzed by SwissADME show compliance with Lipinski's Rule of Five, with 0 violations, while compounds (GDM26, GDM35, and GDM24) show 1 violation. These findings imply that the substances are likely to be well absorbed from the digestive system and have advantageous qualities for oral administration. Compounds do not cause any PAINS alarms, which suggests that they are unlikely to cause non-specific binding interference in biological studies. This is a good result for drug development and discovery. Based on their molecular weight and log *P*, the compounds (GDM22, GDM30, GDM20, GDM29,

GDM31, GDM18, and GDM32) are lead-like, suggesting that they could be a good place to start for additional optimization. However, GDM26 (2 violations), GDM35 (1 violations), GDM27 (1 violations), and GDM24 (2 violations) raise the possibility of some difficulties or space for improvement as the compounds are optimized for use in drug development. It is recommended to pursue experimental validation and structural optimization to overcome any constraints and validate the drug candidate's suitability.

SwissADME and other computational tools are very helpful in the early phases of drug discovery, but they are not flawless. Understanding the limitations of these instruments is crucial, and a more precise and reliable evaluation of a compound's drug-likeness and pharmacokinetic behavior is ensured by combining computational predictions with (pre)clinical experiments and trials. Drug development can be more successfully accomplished by bridging the gap between theoretical predictions and useful, practical outcomes through experimental validation.

4.4.3. Antibacterial activity

The resulting compounds were evaluated against clinically relevant bacterial strains in an *in vitro* microdilution experiment. The antibacterial activity is given in μM using the MIC method. The MIC values were examined following 24 and 48 hours of incubation. For every pathogen, the MIC values acquired from the two time points were all insignificant. None of the tested compounds demonstrated significant activity at the highest tested concentration of 500 μM for compounds that were sufficiently soluble in the testing conditions, despite the fact that the title compounds were intended to be antistaphylococcal agents. Results are summarized in table 10 below. MIC values for standards used for antibacterial evaluation are shown in table 11.

Table 10: The antibacterial properties of the final compounds are expressed in μM for MIC/IC95.

		MIC/IC ₉₅ (μM)								
		GDM29	GDM32	GDM31	GDM20	GDM22	GDM30	GDM27	GDM35	GDM26
SA	24h	>125	>125	>500	>125	>500	>125	>125	>125	62.5
	48h	>125	>125	>500	>125	>500	>125	>125	>125	125
MRSA	24h	>125	>125	>500	>125	>500	>125	>125	>125	>125
	48h	>125	>125	>500	>125	>500	>125	>125	>125	>125
SE	24h	>125	>125	>500	>125	>500	>125	>125	>125	>125
	48h	>125	>125	>500	>125	>500	>125	>125	>125	>125
EF	24h	>125	>125	>500	>125	>500	>125	>125	>125	>125
	48h	>125	>125	>500	>125	>500	>125	>125	>125	>125
EC	24h	>125	>125	>500	>125	>500	>125	>125	>125	>125
	48h	>125	>125	>500	>125	>500	>125	>125	>125	>125
KP	24h	>125	>125	>500	>125	>500	>125	>125	>125	>125
	48h	>125	>125	>500	>125	>500	>125	>125	>125	>125
ACI	24h	>125	>125	>500	>125	>500	>125	>125	>125	>125
	48h	>125	>125	>500	>125	>500	>125	>125	>125	>125
PA	24h	>125	>125	>500	>125	>500	>125	>125	>125	>125
	48h	>125	>125	>500	>125	>500	>125	>125	>125	>125

Note: Bacterial strains listed in the table are as follows: SA = *Staphylococcus aureus* subsp. *aureus* ATCC 29213, CCM 4223 MRSA = *Staphylococcus aureus* subsp. *aureus* ATCC 43300, CCM 4750 SE = *Staphylococcus epidermidis* ATCC 12228, CCM 4418 EF = *Enterococcus faecalis* ATCC 29212, CCM 4224 EC = *Escherichia coli* ATCC 25922, CCM 3954 KP = *Klebsiella pneumoniae* ATCC 10031, CCM 4415 ACI = *Acinetobacter baumannii* ATCC 19606, DSM 30007 PA = *Pseudomonas aeruginosa* ATCC 27853, CCM 3955

Table 11: MIC values of standards used in antibacterial activity evaluation assay expressed in μM . CIP stands for ciprofloxacin. GNT stands for gentamicin.

Standard	SA	MIRSA	SE	EF	EC	KP	ACI	PA	
	48h	48h	48h	48h	48h	48h	48h	72h	120h
CIP	0.256	0.128	0.128	0.512	0.008	0.008	0.512	-	0.512
GNT	1	1	0.125	>8	1	0.5	4	-	0.5

4.4.4. Antimycobacterial Activity

The final compounds were assessed for their antimycobacterial activity against the pathogenic, slow-growing strains as a supplementary test. The MIC values against the avirulent strain of *Mtb* H37Ra are reported in the literature to be qualitatively identical to the MIC values against the virulent strain of *Mtb* H37Rv.[79] As a result, the highly pathogenic *Mtb* H37Rv is substituted for the avirulent strain *Mtb* H37Ra in study. Conversely, *M. smegmatis* and *M. aurum* are fast-growing mycobacteria that only infect immunocompromised people. These two mycobacterial species are also surrogate organisms since they resemble *Mtb* H37Rv in terms of resistance profile and cell wall structure.[80]. The minimal inhibitory concentration (MIC) of antimycobacterial activity is expressed in $\mu\text{g}/\text{mL}$ and is shown in Table 12. According to their lipophilicity (log P value), compounds are arranged in the table in ascending order. MIC = 62.5 $\mu\text{g}/\text{mL}$ is the activity cutoff, below which activity is deemed significant.

Table 12: Antimycobacterial activity of the final compounds are expressed in μM for MIC/IC95.

Cmp d.	CODE	R	logP	Antimycobacterial Activity MIC in $\mu\text{g}/\text{mL}$					
				<i>Mtb</i> H37Rv	<i>Mtb</i> H37Ra	<i>M. kansasii</i>	<i>M. avium</i>	<i>M. smeg</i>	<i>M. aurum</i>
1	GDM18	4-OH	3.11	>100	62.5	62.5	62.5	62.5	62.5
2	GDM29	2,4-di-OCH ₃	3.25	>100	≥ 125	≥ 125	≥ 125	≥ 125	≥ 125
3	GDM32	3-OCH ₃	3.38	>100	62.5	7.81	≥ 500	≥ 125	≥ 125
4	GDM31	4-OCH ₃	3.38	>100	7.81	7.81	≥ 500	31.25	15.625
5	GDM20	2-F	3.66	>100	≥ 500	7.81	≥ 500	≥ 500	≥ 500
6	GDM22	4-F	3.66	25	250	3.91	15.625	31.25	31.25
7	GDM30	2-CH ₃	3.99	>100	≥ 250	≥ 250	≥ 250	≥ 250	≥ 250
8	GDM27	3-Cl	4.09	25	≥ 250	3.91	≥ 250	≥ 250	≥ 250
9	GDM24	4-CF ₃	4.42	>100	125	7.81	≥ 500	≥ 500	≥ 500
10	GDM35	naphthyl	4.5	>100	≥ 125	62.5	≥ 125	≥ 125	≥ 125
11	GDM26	3,4-diCl	4.62	>100	15.625	3.91	≥ 125	≥ 125	≥ 125
INH			-0.64	0.2	0.25	6.25	1000	15.625	3.91
RIF			4.24	n.a.	0.0015625	0.025	0.125	12.5	0.39
CIP			1.32	n.a.	0.25	0.25	1.56	0.125	0.015625

According to the results shown in the table above, we find that most compounds exerted potent antimycobacterial activity against *M. kansasii*, with compounds GDM22 (R = 4-F), GDM27 (R = 3-Cl), and GDM26 (R = 3,4-diCl) being most active with MIC = 3.91 $\mu\text{g}/\text{mL}$. On the other hand, activities against *Mtb* H37Rv and *Mtb* H37Ra are not in sync; compounds GDM22 (R = 4-F) and GDM27 (R = 3-Cl) had marginal activity against *Mtb* H37Rv (MIC = 25 $\mu\text{g}/\text{mL}$) with no activity against *Mtb* H37Ra, and compounds GDM31 (R = 4-OCH₃) and GDM26 (R = 3,4-diCl) had activity against *Mtb* H37Ra but not *Mtb* H37Rv. Such discrepancies may be justified by differences in cellular structures that may affect either penetration (availability) or differences in the end target (mechanism of action).

None of the tested compounds had activity against *M. avium*, with the exception of compound GDM22 (R = 4-F; MIC = 15.625 µg/mL). Only two compounds, namely GDM31 (R = 4-OCH₃) and GDM22 (R = 4-F), exerted activity against *M. smeg* and *M. aurum*, both of which bear substituents at position 4, interestingly of different nature lipophilicity wise. The latter activities make compound GDM22 the broadest spectrum among prepared compounds. The fact that GDM22 is inactive against *Mtb* H37Ra excludes nonspecific toxicity nature.

4.4.5. Antifungal activity

The resulting compounds were evaluated against eight clinically significant fungal strains using a microdilution *in vitro* assay. The antifungal activity is represented in μM by the MIC. All of the MIC values that were mentioned were obtained after 24 and 48 hours of incubation, with the exception of TI, for which the measurements were made after 72 and 120 hours. For every pathogen, the MIC values acquired from the two time points were all insignificant. Results are summarized in table 13 below. MIC values for standards used for antibacterial evaluation are shown in table 14. Among the compounds that were examined, none exhibited significant antifungal action.

Table 13: Antifungal activities of the final compounds are expressed in μM for MIC/IC95.

		MIC/IC ₉₅ (μM)								
		GDM29	GDM32	GDM31	GDM20	GDM22	GDM30	GDM27	GDM35	GDM26
CA	24h	>125	>125	>500	>125	>500	>125	>125	>125	>125
	48h	>125	>125	>500	>125	>500	>125	>125	>125	>125
CK	24h	>125	>125	>500	>125	>500	>125	>125	>125	>125
	48h	>125	>125	>500	>125	>500	>125	>125	>125	>125
CP	24h	>125	>125	>500	>125	>500	>125	>125	>125	>125
	48h	>125	>125	>500	>125	>500	>125	>125	>125	>125
CT	24h	>125	>125	>500	>125	>500	>125	>125	>125	>125
	48h	>125	>125	>500	>125	>500	>125	>125	>125	>125
AF	24h	>125	>125	>500	>125	>500	>125	>125	>125	>125
	48h	>125	>125	>500	>125	>500	>125	>125	>125	>125
AFla	24h	>125	>125	>500	>125	>500	>125	>125	>125	>125
	48h	>125	>125	>500	>125	>500	>125	>125	>125	>125
AC	24h	>125	>125	>500	>125	>500	>125	>125	>125	>125
	48h	>125	>125	>500	>125	>500	>125	>125	>125	>125
TI	5dn ú	>125	>125	>500	>125	>500	>125	>125	>125	>125
	7dn ú	>125	>125	>500	>125	>500	>125	>125	>125	>125

Note: Fungal strains listed in the table are as follows: CA = *Candida albicans* ATCC 24433, CCM 8320 CK = *Candida krusei* ATCC 6258, CCM 8271 CP = *Candida parapsilosis* ATCC 22019, CCM 8260 CT = *Candida tropicalis* ATCC 750, CCM 8264 AF = *Aspergillus fumigatus* ATCC 204305 AFla = *Aspergillus flavus* CCM 8363 AC = *Absidia corymbifera* CCM 8077 TI = *Trichophyton interdigitale* ATCC 9533, CCM 8377

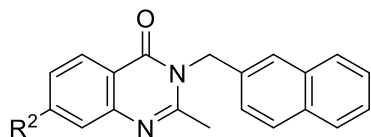
Table 14: MIC values of standards used in antifungal activity evaluation assay expressed in μM . AmB stands for amphotericin B. VRC stands for voriconazole.

Standard	CA	CK	CP	CT	AF	Afla	LC	TI
	48h	48h	48h	48h	48h	48h	48h	120h
AmB	1	1	1	1	4	4	4	8
VRC	>16	16	>16	>16	1	2	>16	>16

Table 15: Antimycobacterial activity is expressed as minimal inhibitory concentration (MIC) in $\mu\text{g/mL}$ for compounds similar to colleague's work. Entries with grey-shaded background represent my work.

CODE	R	logP	Antimycobacterial Activity MIC in $\mu\text{g/mL}$					
			<i>Mtb</i> H37Rv	<i>Mtb</i> H37Ra	<i>M. kansasii</i>	<i>M. avium</i>	<i>M. smeg</i>	<i>M. aurum</i>
GDM29	2,4-diOCH ₃	3.25	>100	≥ 125	≥ 125	≥ 125	≥ 125	≥ 125
GDM12		2.69	>100	≥ 500	15.625	≥ 500	≥ 500	≥ 500
GDM32	3-OCH ₃	3.38	>100	62.5	7.81	≥ 500	≥ 125	≥ 125
GDM15		2.82	100	62.5	15.625	62.5	250	125
GDM31	4-OCH ₃	3.38	>100	7.81	7.81	≥ 500	31.25	15.625
GDM14		2.82	>100	≥ 250	15.625	≥ 250	≥ 250	≥ 250
GDM30	2-CH ₃	3.99	>100	≥ 250	≥ 250	≥ 250	≥ 250	≥ 250
GDM13		3.43	>100	≥ 500	15.625	≥ 500	≥ 500	≥ 500
GDM27	3-Cl	4.09	25	≥ 250	3.91	≥ 250	≥ 250	≥ 250
GDM10		3.5	50	31.25	7.81	31.25	62.5	62.5
GDM24	4-CF ₃	4.42	>100	125	7.81	≥ 500	≥ 500	≥ 500
GDM7		3.86	>100	62.5	62.5	125	250	125
GDM35	See structure below	4.5	>100	≥ 125	62.5	≥ 125	≥ 125	≥ 125
GDMN		3.94	>100	≥ 250	15.625	62.5	≥ 500	62.5
GDM26	3,4-diCl	4.62	>100	15.625	3.91	≥ 125	≥ 125	≥ 125
GDM9		4.06	>100	≥ 250	15.625	≥ 250	≥ 250	≥ 250

* The structure of GDM35 ($R^2 = \text{Cl}$) / GDMN ($R^2 = \text{H}$) is



5. CONCLUSIONS

All things considered, the study presented in this diploma thesis was originally meant to be a component of a broader series of compounds that would have biological activity against the pathogenic bacteria *Staphylococcus aureus* (SA). Using data from the literature on antistaphylococcal quinazolinones that target SA penicillin binding protein (PBP) 2a and in silico docking studies conducted by other members of our research group, the chemical structure of the lead parent drug was created. Ten final compounds with variable lipophilicity and log P values ranging from 3.11 to 4.5 were produced by reacting the lactone intermediate 7-chlorobenzoxazinone with different benzyl amines. A series closely related to this one by another diploma student [81] did not have a chlorine atom at position 7 of the quinazolinone ring, and final compounds bearing matching substituents were compared to them. We used the Royal Society of Chemistry's (RSC) publicly available online ChemSpider tool (www.chemspider.com) to confirm the unique properties of our completed compounds. None of the title compounds, according to the ChemSpider tool, had a ChemSpider identifier number and had not been synthesized or reviewed before, based on searches conducted in the PubMed and RSC journals. Despite being intended as antistaphylococcal active agents, none of the final compounds demonstrated significant antistaphylococcal activity. The final compounds were assessed in a supplementary testing procedure against a panel that included extra pathogens, which comprised certain mycobacteria, fungi, and gram-positive and gram-negative bacteria. The majority of these compounds had strong antimycobacterial activity against *M. kansasii*; the most active compounds were GDM22 (R = 4-F), GDM27 (R = 3-Cl), and GDM26 (R = 3,4-diCl), with MIC values of 3.91 µg/mL. Compounds GDM22 (R = 4-F) and GDM27 (R = 3-Cl) had marginal activity against *Mtb* H37Rv (MIC = 25 µg/mL) with no activity against *Mtb* H37Ra, while compounds GDM31 (R = 4-OCH₃) and GDM26 (R = 3,4-diCl) had activity against *Mtb* H37Ra but not against *Mtb* H37Rv. Only two drugs have demonstrated activity against *M. smegmatis* and *M. aurum*: GDM31 (R = 4-OCH₃) and GDM22 (R = 4-F). Interestingly, substituents are present in both molecules at position 4, while their lipophilicity properties differ. Among the prepared compounds, compound GDM22 had the widest spectrum due to the latter activities. Nonspecific toxicity was ruled out by GDM22's inactivity against *Mtb* H37Ra. Our outcomes imply that the focus of such design should be shifted away from SA and more toward mycobacteria. Future research will look at whether the active compounds' target is the mycobacterial penicillin binding protein. It must be noted -and as stated earlier- that title compounds are part of a larger series of compounds designed to target SA, yet in the original design, these compounds shall serve as intermediates to prepare other final compounds. This explains why we have a methyl group for example in position 3, while according to established SAR from the literature, there should be a bulkier substituent (a substituted aromatic ring) as shown earlier in text in Figure 3. Therefore, future plans include using compounds reported in this work to prepare others and then reevaluate them for their biological activities.

6. ABSTRAKT (CZECH)

Univerzita Karlova, Farmaceutická fakulta v HRadci Králové

Katedra farmaceutické chemie a farmaceutické analýzy

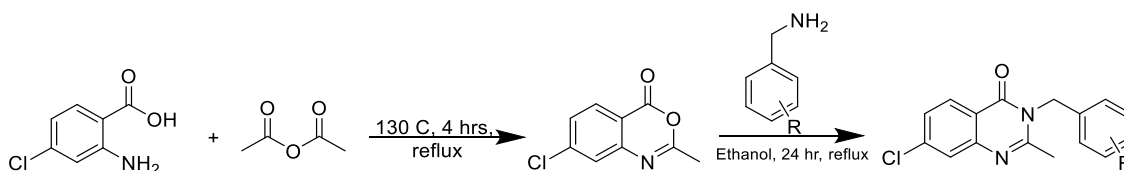
Autor: Hanieh Kamangar

Školitel: doc. PharmDr. Jan Zitko, Ph.D.

Konzultant: Ghada Bouz, Ph.D.

Název diplomové práce: Syntéza a hodnocení nových chinazolonů jako potenciálních antimikrobních sloučenin

Staphylococcus aureus (SA) je převládající bakterie, která může způsobit mírné i život ohrožující infekce. Vývoj nových látek s jedinečným způsobem působení proti kmenům citlivým na léky a rezistentním na léky je nezbytností pro zvládnutí šíření SA infekcí. Quinazolinonová část funguje jako základní stavební blok pro řadu biologicky aktivních látek. V literatuře byly stanoveny vztahy mezi strukturou a aktivitou pro antistafylokokové chinazolony (AQ). AQ se zaměřují na několik molekulárních cílů, včetně laktátdehydrogenázy, DNA topoizomerázy a proteinu vázajícího penicilin (PBP). Zkombinovali jsme naše široké znalosti antibakteriálních látek s publikovanou literaturou pomocí in silico docking, abychom vytvořili nové, potenciálně účinné AQ, které se specificky zaměřují na PBP 2a. Výsledkem bylo, že jsme nechali reagovat laktonový meziproduct, 7-chlorbenzoxazinon, s různými benzylaminy za vzniku 10 konečných sloučenin v rozmezí parametru lipofility logP od 3,11 do 4,5. Žádná z konečných sloučenin nevykazovala významnou antistafylokokovou aktivitu, navzdory jejich původnímu návrhu jako antistafylokoková aktivní činidla. Finální sloučeniny byly hodnoceny proti panelu patogenů, který zahrnoval některé grampozitivní a gramnegativní bakterie, mykobakterie a houby, jako doplňkové testování. GDM22 (R = 4-F) patřil mezi neúčinnější sloučeniny proti *M. kansasii* (MIC = 3,91 µg/ml), s rozšířeným spektrem aktivity, včetně *Mtb* H37Rv (MIC = 25 µg/ml), což z něj činí nejslibnější sloučenina. Podle našich výsledků by spíše než SA měly být mykobakterie primárním cílem těchto navrhovaných molekul. Budoucí studie prozkoumají, zda je cílem aktivní sloučeniny mykobakterie, protein vázající penicilin 2a.



R= 2-Me; 3-Cl; 4-OH; 2,4-diMeO; 3-MeO; 4-MeO; 2-F; 4-F; 3,4-diCl; 4-CF₃, etc.

Obrázek 1. Syntetické schéma sloučenin uvedených v názvu.

7. ABSTRACT (ENGLISH)

Charles University, Faculty of Pharmacy in Hradec Králové

Department of Pharmaceutical Chemistry and Pharmaceutical Analysis

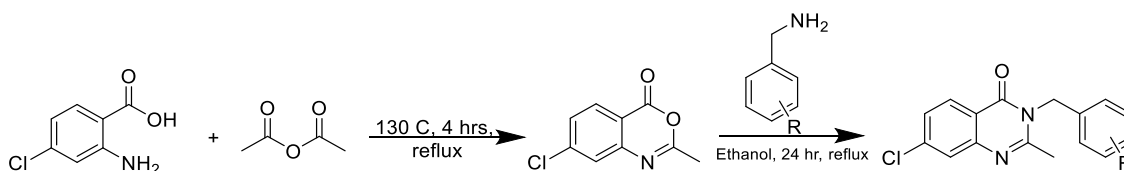
Author: Hanieh Kamangar

Supervisor: Assoc. Prof. PharmDr. Jan Zitko, Ph.D.

Consultant: Ghada Bouz, Ph.D.

Title of diploma thesis: Synthesis and Evaluation of Novel Quinazolones as Potential Antimicrobial Compounds

Staphylococcus aureus (SA) is a prevalent bacterium that can cause both mild and life-threatening infections. Developing new agents with a unique mode of action against drug-sensitive and drug-resistant strains is a necessity for managing the spread of SA infections. Quinazolinone moiety functions as a fundamental building block for numerous biologically active substances. In the literature, structure-activity relationships have been established for antistaphylococcal quinazolones (AQs). AQs target several molecular targets, including lactate dehydrogenase, DNA topoisomerase, and penicillin binding protein (PBP). We combined our broad understanding of antibacterial agents with published literature using *in silico* docking to generate new, potentially effective AQs that specifically target PBP 2a. As a result, we reacted the lactone intermediate, 7-chlorobenzoxazinone, with various benzyl amines to produce 10 final compounds, ranging in lipophilicity parameter logP from 3.11 to 4.5. None of the final compounds exhibited significant antistaphylococcal activity, despite their initial design as antistaphylococcal active agents. Final compounds were evaluated against a panel of pathogens, which included some gram-positive and gram-negative bacteria, mycobacteria, and fungi, as supplemental testing. GDM22 (R =4-F) was among the most active compounds against *M. kansasii* (MIC = 3.91 µg/mL), with extended spectrum of activity, including *Mtb* H37Rv (MIC =25 µg/mL), making it the most promising compound. According to our results, rather than SA, mycobacteria should be the primary target of these suggested molecules. Future studies will explore whether the active compound's target is the mycobacteria penicillin binding protein 2a.



R= 2-Me; 3-Cl; 4-OH; 2,4-diMeO; 3-MeO; 4-MeO; 2-F; 4-F; 3,4-diCl; 4-CF₃, etc.

Figure 1. Synthetic scheme of title compounds.

8. REFERENCES

1. S. Y. C. Tong, J. S. Davis, E. Eichenberger, T. L. Holland, & V. G. Fowler, Staphylococcus aureus Infections: Epidemiology, Pathophysiology, Clinical Manifestations, and Management. *Clinical Microbiology Reviews*, **28** (2015) 603–661. <https://doi.org/10.1128/CMR.00134-14>.
2. World Health Organization, *Antimicrobial resistance: global report on surveillance* (Geneva: World Health Organization, 2014).
3. S. Gatadi, T. V. Lakshmi, & S. Nanduri, 4(3H)-Quinazolinone derivatives: Promising antibacterial drug leads. *European Journal of Medicinal Chemistry*, **170** (2019) 157–172. <https://doi.org/10.1016/j.ejmech.2019.03.018>.
4. J. L. Lister & A. R. Horswill, Staphylococcus aureus biofilms: recent developments in biofilm dispersal. *Frontiers in Cellular and Infection Microbiology*, **4** (2014) 178. <https://doi.org/10.3389/fcimb.2014.00178>.
5. N. K. Archer, M. J. Mazaitis, J. W. Costerton, J. G. Leid, M. E. Powers, & M. E. Shirtliff, Staphylococcus aureus biofilms. *Virulence*, **2** (2011) 445–459. <https://doi.org/10.4161/viru.2.5.17724>.
6. H. Chen, J. Zhang, Y. He, Z. Lv, Z. Liang, J. Chen, P. Li, J. Liu, H. Yang, A. Tao, & X. Liu, Exploring the Role of Staphylococcus aureus in Inflammatory Diseases. *Toxins*, **14** (2022) 464. <https://doi.org/10.3390/toxins14070464>.
7. M. I. Hutchings, A. W. Truman, & B. Wilkinson, Antibiotics: past, present and future. *Current Opinion in Microbiology*, **51** (2019) 72–80. <https://doi.org/10.1016/j.mib.2019.10.008>.
8. W. I. Northern, Discovery of New Antimicrobial Agents using Combinatorial Chemistry. (n.d.).
9. P. Patel, H. Joshi, U. Shah, M. Bapna, & B. Patel, New Generation of Quinazolinone Derivatives as Potent Antimicrobial Agents. *Asian Pacific Journal of Health Sciences*, **8** (2021). <https://doi.org/10.21276/apjhs.2021.8.2.12>.
10. G. V. Asokan, T. Ramadhan, E. Ahmed, & H. Sanad, WHO Global Priority Pathogens List: A Bibliometric Analysis of Medline-PubMed for Knowledge Mobilization to Infection Prevention and Control Practices in Bahrain. *Oman Medical Journal*, **34** (2019) 184–193. <https://doi.org/10.5001/omj.2019.37>.
11. K.-F. Kong, L. Schneper, & K. Mathee, Beta-lactam antibiotics: from antibiosis to resistance and bacteriology. *APMIS: acta pathologica, microbiologica, et immunologica Scandinavica*, **118** (2010) 1–36. <https://doi.org/10.1111/j.1600-0463.2009.02563.x>.
12. B. J. Hartman & A. Tomasz, Low-affinity penicillin-binding protein associated with beta-lactam resistance in Staphylococcus aureus. *Journal of Bacteriology*, **158** (1984) 513–516. <https://doi.org/10.1128/jb.158.2.513-516.1984>.
13. J. D. Pitout, C. C. Sanders, & W. E. Sanders, Antimicrobial resistance with focus on beta-lactam resistance in gram-negative bacilli. *The American Journal of Medicine*, **103** (1997) 51–59. [https://doi.org/10.1016/s0002-9343\(97\)00044-2](https://doi.org/10.1016/s0002-9343(97)00044-2).
14. D. Biek, I. A. Critchley, T. A. Riccobene, & D. A. Thye, Ceftaroline fosamil: a novel broad-spectrum cephalosporin with expanded anti-Gram-positive activity. *The Journal of Antimicrobial Chemotherapy*, **65 Suppl 4** (2010) iv9-16. <https://doi.org/10.1093/jac/dkq251>.
15. J. Fishovitz, J. A. Hermoso, M. Chang, & S. Mobashery, Penicillin-Binding Protein 2a of Methicillin-Resistant Staphylococcus aureus. *IUBMB life*, **66** (2014) 572–577. <https://doi.org/10.1002/iub.1289>.
16. L. H. Otero, A. Rojas-Altuve, L. I. Llarrull, C. Carrasco-López, M. Kumarasiri, E. Lastochkin, J. Fishovitz, M. Dawley, D. Heseck, M. Lee, J. W. Johnson, J. F. Fisher, M. Chang, S. Mobashery, & J. A. Hermoso, How allosteric control of Staphylococcus aureus penicillin binding protein 2a enables methicillin resistance and physiological function. *Proceedings of the National Academy of Sciences of the United States of America*, **110** (2013) 16808–16813. <https://doi.org/10.1073/pnas.1300118110>.

17. K. A. Rodvold & K. W. McConeghy, Methicillin-Resistant *Staphylococcus aureus* Therapy: Past, Present, and Future. *Clinical Infectious Diseases*, **58** (2014) S20–S27. <https://doi.org/10.1093/cid/cit614>.
18. M. Sahre, S. Sabarinath, M. Grant, C. Seubert, C. DeAnda, P. Prokocimer, & H. Derendorf, Skin and soft tissue concentrations of tedizolid (formerly torezolid), a novel oxazolidinone, following a single oral dose in healthy volunteers. *International Journal of Antimicrobial Agents*, **40** (2012) 51–54. <https://doi.org/10.1016/j.ijantimicag.2012.03.006>.
19. K. Bush & P. A. Bradford, β -Lactams and β -Lactamase Inhibitors: An Overview. *Cold Spring Harbor Perspectives in Medicine*, **6** (2016) a025247. <https://doi.org/10.1101/cshperspect.a025247>.
20. A. Torres, A. Kuraieva, G. G. Stone, & C. Cillóniz, Systematic review of ceftaroline fosamil in the management of patients with methicillin-resistant *Staphylococcus aureus* pneumonia. *European Respiratory Review*, **32** (2023) 230117. <https://doi.org/10.1183/16000617.0117-2023>.
21. L. A. Altamimi, L. A. Altamimi, & A. M. Somily, The antimicrobial activity of ceftobiprole against Methicillin-resistant *Staphylococcus aureus* and multi-drug resistant *Pseudomonas aeruginosa*. *Saudi Medical Journal*, **43** (2022) 31–36. <https://doi.org/10.15537/smj.2022.43.1.20210587>.
22. R. Yoo, H. So, E. Seo, M. Kim, & J. Lee, Impact of initial vancomycin pharmacokinetic/pharmacodynamic parameters on the clinical and microbiological outcomes of methicillin-resistant *Staphylococcus aureus* bacteremia in children. *PLoS ONE*, **16** (2021) e0247714. <https://doi.org/10.1371/journal.pone.0247714>.
23. H. Kato, M. Hagihara, N. Asai, Y. Shibata, Y. Koizumi, Y. Yamagishi, & H. Mikamo, Meta-analysis of vancomycin versus linezolid in pneumonia with proven methicillin-resistant *Staphylococcus aureus*. *Journal of Global Antimicrobial Resistance*, **24** (2021) 98–105. <https://doi.org/10.1016/j.jgar.2020.12.009>.
24. J. A. Karlowsky, K. Nichol, & G. G. Zhanel, Telavancin: Mechanisms of Action, In Vitro Activity, and Mechanisms of Resistance. *Clinical Infectious Diseases*, **61** (2015) S58–S68. <https://doi.org/10.1093/cid/civ534>.
25. G. Lin, G. A. Pankuch, L. M. Ednie, & P. C. Appelbaum, Antistaphylococcal Activities of Telavancin Tested Alone and in Combination by Time-Kill Assay. *Antimicrobial Agents and Chemotherapy*, **54** (2010) 2201–2205. <https://doi.org/10.1128/AAC.01143-09>.
26. M. Heidary, A. D. Khosravi, S. Khoshnood, M. J. Nasiri, S. Soleimani, & M. Goudarzi, Daptomycin. *Journal of Antimicrobial Chemotherapy*, **73** (2018) 1–11. <https://doi.org/10.1093/jac/dkx349>.
27. M. Geriak, F. Haddad, K. Rizvi, W. Rose, R. Kullar, K. LaPlante, M. Yu, L. Vasina, K. Ouellette, M. Zervos, V. Nizet, & G. Sakoulas, Clinical Data on Daptomycin plus Ceftaroline versus Standard of Care Monotherapy in the Treatment of Methicillin-Resistant *Staphylococcus aureus* Bacteremia. *Antimicrobial Agents and Chemotherapy*, **63** (2019) e02483-18. <https://doi.org/10.1128/AAC.02483-18>.
28. C. Roger, J. A. Roberts, & L. Muller, Clinical Pharmacokinetics and Pharmacodynamics of Oxazolidinones. *Clinical Pharmacokinetics*, **57** (2018) 559–575. <https://doi.org/10.1007/s40262-017-0601-x>.
29. K. S. Thomson & R. V. Goering, Activity of Tedizolid (TR-700) against Well-Characterized Methicillin-Resistant *Staphylococcus aureus* Strains of Diverse Epidemiological Origins. *Antimicrobial Agents and Chemotherapy*, **57** (2013) 2892–2895. <https://doi.org/10.1128/AAC.00274-13>.
30. P. B. Murphy, K. G. Bistas, P. Patel, & J. K. Le, Clindamycin. *StatPearls* (Treasure Island (FL): StatPearls Publishing, 2024).
31. A. Babiker, X. Li, Y. L. Lai, J. R. Strich, S. Warner, S. Sarzynski, J. P. Dekker, R. L. Danner, & S. S. Kadri, Effectiveness of adjunctive clindamycin in β -lactam antibiotic-treated patients with invasive β -haemolytic streptococcal infections in US hospitals: a retrospective

- multicentre cohort study. *The Lancet. Infectious diseases*, **21** (2021) 697–710. [https://doi.org/10.1016/S1473-3099\(20\)30523-5](https://doi.org/10.1016/S1473-3099(20)30523-5).
32. M. P. Veve & J. L. Wagner, Lefamulin: Review of a Promising Novel Pleuromutilin Antibiotic. *Pharmacotherapy*, **38** (2018) 935–946. <https://doi.org/10.1002/phar.2166>.
 33. W. van Os & M. Zeitlinger, Target attainment of intravenous lefamulin for treatment of acute bacterial skin and skin structure infections. *Journal of Antimicrobial Chemotherapy*, **79** (2024) 443–446. <https://doi.org/10.1093/jac/dkad401>.
 34. S. C. J. Jorgensen, N. J. Mercurio, S. L. Davis, & M. J. Rybak, Delafloxacin: Place in Therapy and Review of Microbiologic, Clinical and Pharmacologic Properties. *Infectious Diseases and Therapy*, **7** (2018) 197–217. <https://doi.org/10.1007/s40121-018-0198-x>.
 35. I. Khan, S. Zaib, S. Batool, N. Abbas, Z. Ashraf, J. Iqbal, & A. Saeed, Quinazolines and quinazolinones as ubiquitous structural fragments in medicinal chemistry: An update on the development of synthetic methods and pharmacological diversification. *Bioorganic & Medicinal Chemistry*, **24** (2016) 2361–2381. <https://doi.org/10.1016/j.bmc.2016.03.031>.
 36. V. Alagarsamy, K. Chitra, G. Saravanan, V. R. Solomon, M. T. Sulthana, & B. Narendhar, An overview of quinazolines: Pharmacological significance and recent developments. *European Journal of Medicinal Chemistry*, **151** (2018) 628–685. <https://doi.org/10.1016/j.ejmech.2018.03.076>.
 37. R. Rajput & A. Mishra, A REVIEW ON BIOLOGICAL ACTIVITY OF QUINAZOLINONES. (2012).
 38. D. J. Fry, J. D. Kendall, & A. J. Morgan, 979. The reactivity of the alkylthio-group in nitrogen ring compounds. Part IV. Quaternary salts of 4-substituted quinazolines. *Journal of the Chemical Society (Resumed)*, (1960) 5062–5072. <https://doi.org/10.1039/JR9600005062>.
 39. J. B. Koepfli, J. F. Mead, & J. A. Brockman, An alkaloid with high antimalarial activity from *Dichroa febrifuga*. *Journal of the American Chemical Society*, **69** (1947) 1837. <https://doi.org/10.1021/ja01199a513>.
 40. B. K. Tiwary, K. Pradhan, A. K. Nanda, & R. Chakraborty, Implication of Quinazoline-4(3H)-ones in Medicinal Chemistry: A Brief Review. *Journal of Chemical Biology & Therapeutics*, **1** (2015) 1–7. <https://doi.org/10.4172/2572-0406.1000104>.
 41. S. B. Mhaske & N. P. Argade, The chemistry of recently isolated naturally occurring quinazolinone alkaloids. *Tetrahedron*, **62** (2006) 9787–9826. <https://doi.org/10.1016/j.tet.2006.07.098>.
 42. M. M. Ghorab, Z. H. Ismail, A. A. Radwan, & M. Abdalla, Synthesis and pharmacophore modeling of novel quinazolines bearing a biologically active sulfonamide moiety. *Acta Pharmaceutica (Zagreb, Croatia)*, **63** (2013) 1–18. <https://doi.org/10.2478/acph-2013-0006>.
 43. M. F. Zayed & M. H. Hassan, Synthesis and biological evaluation studies of novel quinazolinone derivatives as antibacterial and anti-inflammatory agents. *Saudi Pharmaceutical Journal : SPJ*, **22** (2014) 157–162. <https://doi.org/10.1016/j.jsps.2013.03.004>.
 44. Y. A. El-Badry, N. A. Anter, & H. S. El-Sheshtawy, Synthesis and evaluation of new polysubstituted quinazoline derivatives as potential antimicrobial agents | Abstract. (n.d.).
 45. R. S. Dave, R. J. Odedara, R. I. Kalaria, & J. J. Upadhyay, Synthesis, characterization and antimicrobial activity of new quinazolin-4(3H)-one schiff base derivatives. (2012).
 46. K. Devi, M. Sarangapani, & Sriram, Synthesis and Antimicrobial activity of some Quinazolinones Derivatives. *International Journal of Drug Development and Research*, (2012).
 47. M. Al-omar, Synthesis and Biological Screening of Some New Substituted-3H-Quinazolin-4-one Analogs as Antimicrobial Agents. *Saudi ...*, (2005).
 48. K. Ahmed, M. I. Choudhary, & R. S. Z. Saleem, Heterocyclic pyrimidine derivatives as promising antibacterial agents. *European Journal of Medicinal Chemistry*, **259** (2023) 115701. <https://doi.org/10.1016/j.ejmech.2023.115701>.

49. R. D. Smyth, J. K. Lee, A. Polk, P. B. Chemburkar, & A. M. Savacool, Bioavailability of Methaqualone. *The Journal of Clinical Pharmacology and New Drugs*, **13** (1973) 391–400. <https://doi.org/10.1002/j.1552-4604.1973.tb00185.x>.
50. P. Theivendren & P. Kumar, Quinazoline Marketed drugs – A Review. *Res. Pharm.*, **1** (2011) 1–21.
51. J. Hughes, S. Rees, S. Kalindjian, & K. Philpott, Principles of early drug discovery. *British Journal of Pharmacology*, **162** (2011) 1239–1249. <https://doi.org/10.1111/j.1476-5381.2010.01127.x>.
52. L. Sorbera, J. Bartroli, & J. Castañer, Albaconazole. *Drugs of The Future - DRUG FUTURE*, **28** (2003). <https://doi.org/10.1358/dof.2003.028.06.738951>.
53. R. Guillon, F. Pagniez, C. Picot, D. Hédou, A. Tonnerre, E. Chosson, M. Duflos, T. Besson, C. Logé, & P. Le Pape, Discovery of a Novel Broad-Spectrum Antifungal Agent Derived from Albaconazole. *ACS Medicinal Chemistry Letters*, **4** (2013) 288–292. <https://doi.org/10.1021/ml300429p>.
54. J. L. Miller, W. A. Schell, E. A. Wills, D. L. Toffaletti, M. Boyce, D. K. Benjamin, J. Bartroli, & J. R. Perfect, In vitro and in vivo efficacies of the new triazole albaconazole against *Cryptococcus neoformans*. *Antimicrobial Agents and Chemotherapy*, **48** (2004) 384–387. <https://doi.org/10.1128/AAC.48.2.384-387.2004>.
55. M. S. Sundrud, S. B. Korolov, M. Feuerer, D. P. Calado, A. E. Kozhaya, A. Rhule-Smith, R. E. Lefebvre, D. Unutmaz, R. Mazitschek, H. Waldner, M. Whitman, T. Keller, & A. Rao, Halofuginone Inhibits TH17 Cell Differentiation by Activating the Amino Acid Starvation Response. *Science (New York, N.Y.)*, **324** (2009) 1334–1338. <https://doi.org/10.1126/science.1172638>.
56. A. Lamora, M. Mullard, J. Amiaud, R. Brion, D. Heymann, F. Redini, & F. Verrecchia, Anticancer activity of halofuginone in a preclinical model of osteosarcoma: inhibition of tumor growth and lung metastases. *Oncotarget*, **6** (2015) 14413–14427.
57. Y. Murase, H. Ono, K. Ogawa, R. Yoshioka, Y. Ishikawa, H. Ueda, K. Akahoshi, D. Ban, A. Kudo, S. Tanaka, & M. Tanabe, Inhibitor library screening identifies ispinesib as a new potential chemotherapeutic agent for pancreatic cancers. *Cancer Science*, **112** (2021) 4641–4654. <https://doi.org/10.1111/cas.15134>.
58. S. P. Blagden, L. R. Molife, A. Seebaran, M. Payne, A. H. M. Reid, A. S. Protheroe, L. S. Vasist, D. D. Williams, C. Bowen, S. J. Kathman, J. P. Hodge, M. M. Dar, J. S. de Bono, & M. R. Middleton, A phase I trial of ispinesib, a kinesin spindle protein inhibitor, with docetaxel in patients with advanced solid tumours. *British Journal of Cancer*, **98** (2008) 894–899. <https://doi.org/10.1038/sj.bjc.6604264>.
59. E. Cohen, B. Klarberg, & J. R. Jr. Vaughan, Quinazolinone Sulfonamides. A New Class of Diuretic Agents¹. *Journal of the American Chemical Society*, **82** (1960) 2731–2735. <https://doi.org/10.1021/ja01496a020>.
60. G. Sandler, Quinethazone, a New Oral Diuretic. *British Medical Journal*, **2** (1964) 288–292.
61. M. Dvorakova, L. Langhansova, V. Temml, A. Pavicic, T. Vanek, & P. Landa, Synthesis, Inhibitory Activity, and In Silico Modeling of Selective COX-1 Inhibitors with a Quinazoline Core. *ACS Medicinal Chemistry Letters*, **12** (2021) 610–616. <https://doi.org/10.1021/acsmchemlett.1c00004>.
62. H. Hammer, B. M. Bader, C. Ehnert, C. Bundgaard, L. Bunch, K. Hoestgaard-Jensen, O. H.-U. Schroeder, J. F. Bastlund, A. Gramowski-Voß, & A. A. Jensen, A Multifaceted GABAA Receptor Modulator: Functional Properties and Mechanism of Action of the Sedative-Hypnotic and Recreational Drug Methaqualone (Quaalude). *Molecular Pharmacology*, **88** (2015) 401–420. <https://doi.org/10.1124/mol.115.099291>.
63. S. N. Murthy Boddapati, H. Babu Bollikolla, K. Geetha Bhavani, H. Singh Saini, N. Ramesh, & S. Babu Jonnalagadda, Advances in synthesis and biological activities of

- quinazoline scaffold analogues: A review. *Arabian Journal of Chemistry*, **16** (2023) 105190. <https://doi.org/10.1016/j.arabjc.2023.105190>.
64. K. Chen, K. Wang, A. M. Kirichian, A. F. Al Aowad, L. K. Iyer, S. J. Adelstein, & A. I. Kassis, In silico design, synthesis, and biological evaluation of radioiodinated quinazolinone derivatives for alkaline phosphatase-mediated cancer diagnosis and therapy. *Molecular Cancer Therapeutics*, **5** (2006) 3001–3013. <https://doi.org/10.1158/1535-7163.MCT-06-0465>.
65. P. S. Auti, G. George, & A. T. Paul, Recent advances in the pharmacological diversification of quinazoline/quinazolinone hybrids. *RSC Advances*, **10** (n.d.) 41353–41392. <https://doi.org/10.1039/d0ra06642g>.
66. S. O. Meroueh, K. Z. Bencze, D. Heseck, M. Lee, J. F. Fisher, T. L. Stemmler, & S. Mobashery, Three-dimensional structure of the bacterial cell wall peptidoglycan. *Proceedings of the National Academy of Sciences of the United States of America*, **103** (2006) 4404–4409. <https://doi.org/10.1073/pnas.0510182103>.
67. T. D. Bugg & C. T. Walsh, Intracellular steps of bacterial cell wall peptidoglycan biosynthesis: enzymology, antibiotics, and antibiotic resistance. *Natural Product Reports*, **9** (1992) 199–215. <https://doi.org/10.1039/np9920900199>.
68. D.-J. Scheffers & M. G. Pinho, Bacterial Cell Wall Synthesis: New Insights from Localization Studies. *Microbiology and Molecular Biology Reviews*, **69** (2005) 585–607. <https://doi.org/10.1128/MMBR.69.4.585-607.2005>.
69. E. Sauvage, F. Kerff, M. Terrak, J. A. Ayala, & P. Charlier, The penicillin-binding proteins: structure and role in peptidoglycan biosynthesis. *FEMS Microbiology Reviews*, **32** (2008) 234–258. <https://doi.org/10.1111/j.1574-6976.2008.00105.x>.
70. D. J. Tipper & J. L. Strominger, Mechanism of action of penicillins: a proposal based on their structural similarity to acyl-D-alanyl-D-alanine. *Proceedings of the National Academy of Sciences of the United States of America*, **54** (1965) 1133–1141.
71. J. Janardhanan, R. Bouley, S. Martínez-Caballero, Z. Peng, M. Batuecas-Mordillo, J. E. Meisel, D. Ding, V. A. Schroeder, W. R. Wolter, K. V. Mahasenan, J. A. Hermoso, S. Mobashery, & M. Chang, The Quinazolinone Allosteric Inhibitor of PBP 2a Synergizes with Piperacillin and Tazobactam against Methicillin-Resistant Staphylococcus aureus. *Antimicrobial Agents and Chemotherapy*, **63** (2019) 10.1128/aac.02637-18. <https://doi.org/10.1128/aac.02637-18>.
72. D. E. Nawrot, G. Bouz, O. Jandourek, K. Konečná, P. Paterová, P. Bárta, M. Novák, R. Kučera, J. Zemanová, M. Forbak, J. Korduláková, O. Pavliš, P. Kubíčková, M. Doležal, & J. Zitko, Antimycobacterial pyridine carboxamides: From design to *in vivo* activity. *European Journal of Medicinal Chemistry*, **258** (2023) 115617. <https://doi.org/10.1016/j.ejmech.2023.115617>.
73. A. Daina, O. Michielin, & V. Zoete, SwissADME: a free web tool to evaluate pharmacokinetics, drug-likeness and medicinal chemistry friendliness of small molecules. *Scientific Reports*, **7** (2017) 42717. <https://doi.org/10.1038/srep42717>.
74. S. Tian, J. Wang, Y. Li, D. Li, L. Xu, & T. Hou, The application of *in silico* drug-likeness predictions in pharmaceutical research. *Advanced Drug Delivery Reviews*, **86** (2015) 2–10. <https://doi.org/10.1016/j.addr.2015.01.009>.
75. R. Brenk, A. Schipani, D. James, A. Krasowski, I. H. Gilbert, J. Frearson, & P. G. Wyatt, Lessons Learnt from Assembling Screening Libraries for Drug Discovery for Neglected Diseases. *Chemmedchem*, **3** (2008) 435–444. <https://doi.org/10.1002/cmdc.200700139>.
76. A. Daina & V. Zoete, A BOILED-Egg To Predict Gastrointestinal Absorption and Brain Penetration of Small Molecules. *Chemmedchem*, **11** (2016) 1117–1121. <https://doi.org/10.1002/cmdc.201600182>.
77. F. Montanari & G. F. Ecker, Prediction of drug-ABC-transporter interaction — Recent advances and future challenges. *Advanced drug delivery reviews*, **86** (2015) 17–26. <https://doi.org/10.1016/j.addr.2015.03.001>.

78. J. B. Baell & G. A. Holloway, New substructure filters for removal of pan assay interference compounds (PAINS) from screening libraries and for their exclusion in bioassays. *Journal of Medicinal Chemistry*, **53** (2010) 2719–2740. <https://doi.org/10.1021/jm901137j>.
79. M. T. Heinrichs, R. J. May, F. Heider, T. Reimers, S. K. B Sy, C. A. Peloquin, & H. Derendorf, Mycobacterium tuberculosis Strains H37ra and H37rv have equivalent minimum inhibitory concentrations to most antituberculosis drugs. *International Journal of Mycobacteriology*, **7** (2018) 156–161. https://doi.org/10.4103/ijmy.ijmy_33_18.
80. S. Sood, A. Yadav, & R. Shrivastava, Mycobacterium aurum is Unable to Survive Mycobacterium tuberculosis Latency Associated Stress Conditions: Implications as Non-suitable Model Organism. *Indian Journal of Microbiology*, **56** (2016) 198–204. <https://doi.org/10.1007/s12088-016-0564-x>.
81. Askari, A. (2024). *Design, synthesis and evaluation of heterocyclic compounds with potential antimicrobial activity* [Master's Diploma Thesis, Faculty of Pharmacy, Charles University].CU Digital Repository. <https://dspace.cuni.cz/handle/20.500.11956/190217?locale-attribute=en>